

Optimization on Manifolds: A Symplectic Approach

Guilherme França,^{a*} Alessandro Barp,^{bc†}
Mark Girolami,^{bc‡} and Michael I. Jordan^{a§}

^a*University of California, Berkeley, USA*

^b*University of Cambridge, Cambridge, UK*

^c*Alan Turing Institute, London, UK*

Abstract

Optimization tasks are crucial in statistical machine learning. Recently, there has been great interest in leveraging tools from dynamical systems to derive accelerated and robust optimization methods via suitable discretizations of continuous-time systems. However, these ideas have mostly been limited to Euclidean spaces and unconstrained settings, or to Riemannian gradient flows. In this work, we propose a dissipative extension of Dirac’s theory of constrained Hamiltonian systems as a general framework for solving optimization problems over smooth manifolds, including problems with nonlinear constraints. We develop geometric/symplectic numerical integrators on manifolds that are “rate-matching,” i.e., preserve the continuous-time rates of convergence. In particular, we introduce a dissipative RATTLE integrator able to achieve optimal convergence rate locally. Our class of (accelerated) algorithms are not only simple and efficient but also applicable to a broad range of contexts.

*guifranca@gmail.com

†ab2286@cam.ac.uk

‡mgirolami@turing.ac.uk

§jordan@cs.berkeley.edu

Contents

1	Introduction	1
2	General Framework	3
2.1	Nonconservative and constrained Hamiltonian systems	3
2.2	Symplectification	3
2.3	Presymplectic integrators	5
3	Dissipative Geodesic under Constraints	6
4	General KKT Conditions on Manifolds	8
5	Dissipative RATTLE for Constrained Optimization	9
6	Numerical Example	10
7	Conclusion	11
A	Review of Conservative Hamiltonian Systems	12
B	The Dissipative Constrained Geodesic Equation	13
C	Shadow Property	14
C.1	Proof of Theorem 5	14
C.2	Proof of Corollary 6	15
D	KKT Conditions and Stability	16
D.1	Proof of Theorem 7	16
D.2	Extension to inequality constraints	17
D.3	Proof of Theorem 8	17
E	Implicit Dynamics on the Constraint Surface and Convergence Rate	18
E.1	Proof of Theorem 9	20
F	Derivation of Dissipative RATTLE for Constrained Optimization	21
F.1	Dissipative RATTLE	22
F.2	Dissipative geodesic RATTLE	23
F.3	Numerical stability	26
G	Optimization over Lie Groups	26
G.1	Dissipative Leapfrog over Lie Groups	27
H	Numerical Details for SSK	29
H.1	SSK over $SO(n)$	30
I	Orthogonal Procrustes Problem	31

1 Introduction

We are interested in constructing a general framework for solving optimization problems of the form

$$\min_{\mathbf{q} \in \mathcal{Q}} f(\mathbf{q}), \quad (1.1)$$

where \mathcal{Q} is a smooth manifold, called *configuration manifold*, and $f : \mathcal{Q} \rightarrow \mathbb{R}$ is a smooth function. Such problems have important applications in machine learning, statistics, and applied mathematics, including maxcut problems, phase retrieval, linear and nonlinear eigenvalue problems, principal component analysis, clustering, and dimensionality reduction, to mention a few examples. Configuration manifolds arise from rank and orthogonality constraints, leading to nonconvex problems.

The geometry of \mathcal{Q} is usually specified by a Riemannian metric. However, for practical reasons, e.g., to avoid computing affine connections or parallel transports, it is convenient to embed \mathcal{Q} into a higher dimensional manifold, which can be taken to be the Euclidean space \mathbb{R}^n . The problem can thus be redefined as minimizing f subject to a set of independent constraints,

$$\min_{\mathbf{q} \in \mathbb{R}^n} f(\mathbf{q}) \quad \text{s.t.} \quad \boldsymbol{\psi}(\mathbf{q}) = \mathbf{0}, \quad (1.2)$$

where $\boldsymbol{\psi} \equiv (\psi_1, \dots, \psi_m) : \mathbb{R}^n \rightarrow \mathbb{R}^m$, $\psi_a : \mathbb{R}^n \rightarrow \mathbb{R}$, $a = 1, \dots, m$. The configuration manifold is a d -dimensional ($d = n - m$) submanifold embedded into \mathbb{R}^n , namely $\mathcal{Q} \equiv \{\mathbf{q} \in \mathbb{R}^n \mid \boldsymbol{\psi}(\mathbf{q}) = \mathbf{0}\}$. Whitney's embedding theorem ensures that any smooth real d -dimensional manifold embeds into \mathbb{R}^{2d} . Also, Nash's embedding theorem ensures that every Riemannian manifold can be isometrically embedded into \mathbb{R}^n for sufficiently large n . Therefore, there is no loss of generality in this approach.

To solve problem (1.2) we need to specify a dynamics whose trajectories asymptotically converge to critical points, i.e., satisfy the Karush–Kuhn–Tucker (KKT) conditions. To this end, we propose a *dissipative* extension of Dirac's theory of constrained Hamiltonian systems [1–3]. The dynamics is of second order and naturally accelerated in a physical sense. We indeed prove that such a system is asymptotically stable and achieves optimal convergence rate near isolated critical points. Furthermore, we generalize problem (1.2) over a Riemannian manifold \mathcal{M} under equality and inequality constraints,

$$\min_{\mathbf{q} \in \mathcal{M}} f(\mathbf{q}) \quad \text{s.t.} \quad \boldsymbol{\psi}(\mathbf{q}) = \mathbf{0}, \quad \boldsymbol{\phi}(\mathbf{q}) \leq \mathbf{0}, \quad (1.3)$$

and propose a suitable dynamics for it.

Our approach is different, and in a sense complementary, to that traditionally found in the optimization literature [4–10]. These approaches invariably rely on the Riemannian geometry of \mathcal{Q} , employing (approximations of) the geodesic or gradient flow. This is valid once a Riemannian metric is specified. In practice, however, this can only be done efficiently for a handful of manifolds with invariant Riemannian metrics. Moreover, geodesic computations take place on the *tangent bundle* $T\mathcal{Q}$, having the undesired effect of moving states off the manifold; some projection back to \mathcal{Q} is often necessary, which can lead to numerical inefficiencies. Alternatively, the *canonical way* to define a dynamics on \mathcal{Q} is through a *Hamiltonian system*, whose phase space is instead the *cotangent bundle* $T^*\mathcal{Q}$. This is because the cotangent bundle of *any* smooth manifold is itself a *symplectic manifold*; a dynamics that preserves the symplectic structure must be Hamiltonian [11]. In other words, a Hamiltonian system naturally respects and is adapted to the geometry of the configuration manifold. Furthermore, through an embedding via constraints, we do not need to rely on the Riemannian metric of \mathcal{Q} .

Relations between Hamiltonian systems and optimization on Euclidean spaces have been attracting great interest; see, e.g., [12–18] and references therein. However, connections with Hamiltonian systems over general smooth manifolds, or with constrained Hamiltonian systems, have not yet been explored. It is the goal of this paper to fill this important gap.

Once a suitable dynamics has been identified, one needs to introduce discretizations that are stable and retain its important properties. Symplectic integrators are the preferred choice for simulating Hamiltonian systems due to their long term stability, for exactly preserving the symplectic structure, and for having close energy conservation [19–23]. However, symplectic integrators were developed for conservative systems. Recently, an extension of symplectic integrators to dissipative settings, yielding methods that closely preserve continuous-time rates, was proposed [24]. This framework again applies to Euclidean and unconstrained settings. Here we further extend these ideas to arbitrary smooth manifolds and for constrained cases, thereby significantly enlarging the range of applications that include problems not only in machine learning and optimization but also in molecular dynamics, control theory, complex systems, and statistical physics. We therefore provide a first principles derivation—based on symplectic geometry and backward error analysis—of manifold/constrained optimization methods that emulate dissipative Hamiltonian systems. Such discretizations preserve the continuous-time rates of convergence via the preservation of a *presymplectic* structure.

The main contributions of this paper are shortly summarized as follows:

- We provide a general framework based on continuous-time systems for optimization on smooth manifolds as well as for problems with nonlinear equality/inequality constraints. This is done by a dissipative extension of Dirac’s theory of constrained Hamiltonian systems.
- We extend the theory of symplectic integrators to construct practical optimization algorithms to this manifold/constrained setting that are “rate-matching.”
- We introduce a system that satisfies the KKT conditions (on curved spaces) and have optimal rates of convergence locally, i.e., accelerated rates sufficiently close to critical points.
- We derive a simple and efficient algorithm that consists of a dissipative generalization of the famous RATTLE integrator from molecular dynamics (our framework allows a variety of other methods to be obtained as well, and we provide extensions in the Appendix).

The outline of the paper is the following. In Sec. 2, we introduce dissipative and constrained Hamiltonian systems over Riemannian manifolds, emphasizing their *symplectification*, which plays a fundamental role for introducing our class of presymplectic integrators. Such discretizations are shown to generalize important properties of symplectic integrators (shadowing). In Sec. 3, we propose a dissipative geodesic equation with equality constraints, and show stability and local (accelerated) convergence rate results. In Sec. 4, we argue that this can be extended to inequality constraints, leading to a general dynamics in consistency with KKT conditions on Riemannian manifolds. In Sec. 5, we state an extension of RATTLE for constrained optimization, with numerical experiments shown in Sec. 6. We conclude in Sec. 7. Note that this paper assumes sufficient background on differential geometry and Hamiltonian systems. Nevertheless, we provide a quick review of basic concepts in the Appendix, which also contains all the technical proofs, omissions, and several additional results not stated in the main part of the paper.

Notation. We refer to vectors in boldface, $\mathbf{q} \in \mathbb{R}^n$, and its components are denoted by q^i , for $i = 1, \dots, n$ (upper indices). The dual or covector $\mathbf{p} \in \mathbb{R}^n$ has components p_i , for $i = 1, \dots, n$ (lower indices). The metric tensor g of type $(2, 0)$ has components g_{ij} , and its inverse g^{-1} , which is a tensor of type $(0, 2)$, has components g^{ij} . We interchangeably refer to vector valued functions as $f(\mathbf{q})$ or $f(q^i)$. The gradient $\nabla f(\mathbf{q})$ has components $\partial_i f$ (covector), where $\partial_i \equiv \partial/\partial q^i$. We use Einstein's summation on repeated upper and lower indices, e.g., $q^i p_i \equiv \sum_{i=1}^n q^i p_i$, $\lambda^a \psi_a \equiv \sum_{a=1}^m \lambda^a \psi_a$, $g^{ij} p_j \equiv \sum_{j=1}^n g^{ij} p_j$, etc. The symbol \wedge denotes the exterior product between differential forms. For simplicity, we often omit variable dependencies, e.g., the function $H(t, q^i, p_i)$ may be denoted simply by H , and $\psi_a(q^i)$ by ψ_a . Other necessary terminologies will be introduced along the paper.

2 General Framework

2.1 Nonconservative and constrained Hamiltonian systems

Let \mathcal{M} be an n -dimensional Riemannian manifold with local coordinates q^i , and let p_i be their conjugate momenta ($i = 1, \dots, n$). We thus have local coordinates $(q^i, p_i) \in \mathbb{R}^{2n}$ on the cotangent bundle $T^*\mathcal{M}$. Let $H(t, \mathbf{q}, \mathbf{p})$ be an unconstrained Hamiltonian function describing some physical system, allowed to be explicit time dependent so as to account for *dissipation*. Consider a set of so-called *primary constraints*, $\psi_a(t, \mathbf{q}, \mathbf{p})$, $a = 1, \dots, m$ [1–3]—in this section we allow the constraints to be more general than actually needed for problem (1.2). A mechanical system subject to these constraints can be defined by the total Hamiltonian

$$H_{\text{total}} \equiv H(t, \mathbf{q}, \mathbf{p}) + \lambda^a \psi_a(t, \mathbf{q}, \mathbf{p}), \quad (2.1)$$

where λ^a are Lagrange multipliers. The constraints define the configuration manifold \mathcal{Q} , which is embedded into \mathcal{M} . Hamilton's equations, $\dot{q}^i = \partial H_{\text{total}}/\partial p_i$ and $\dot{p}^i = -\partial H_{\text{total}}/\partial q^i$, yield

$$\dot{q}^i \approx \frac{\partial H}{\partial p_i} + \lambda^a \frac{\partial \psi_a}{\partial p_i}, \quad \dot{p}^i \approx -\frac{\partial H}{\partial q^i} - \lambda^a \frac{\partial \psi_a}{\partial q^i}. \quad (2.2)$$

We use Dirac's notation [1–3], where \approx means “weak equality” that holds only on the constraint surface $\psi_a(t, \mathbf{q}, \mathbf{p}) = 0$, i.e., it is implicit that the constraint condition is obeyed. The above system is *nonconservative*, $dH_{\text{total}}/dt = \partial H_{\text{total}}/\partial t$, yielding

$$\frac{dH}{dt} \approx \frac{\partial H}{\partial t} \quad (2.3)$$

if we assume that $\partial \psi_a/\partial t \approx 0$. This is an important ingredient, and holds if ψ_a has a factorized form, $\psi_a(t, \mathbf{q}, \mathbf{p}) \mapsto h(t)\psi_a(\mathbf{q}, \mathbf{p})$, for some function $h(t)$, as will be used shortly—note that we always have $d\psi_a/dt \approx 0$ since the constraints are obeyed at all times. If we explicitly solve for the Lagrange multipliers λ^a , which we assume are unique as usual, the differential algebraic equations (2.2) reduce to ordinary differential equations for $2n$ degrees of freedom, which are not all independent, i.e., the phase space of the system is a submanifold $T^*\mathcal{Q} \subset T^*\mathcal{M}$ of codimension $2(n - m)$.

2.2 Symplectification

We now consider a *symplectification* [11], whereby the phase space of the above system can be embedded into a higher dimensional *symplectic manifold*—this will play a fundamental role for

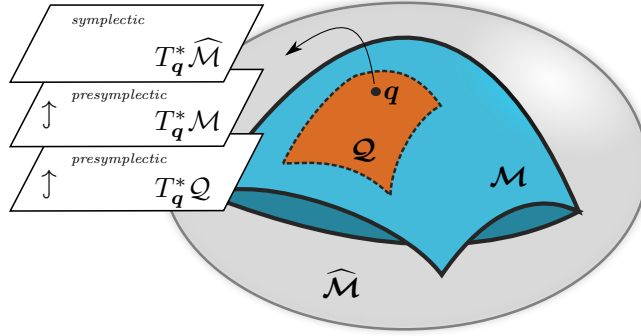


Figure 1: Illustration of the symplectification.

introducing geometric integrators. Thus, we promote time to a new coordinate, $q^0 \equiv t$, and let the Lagrange multipliers λ^a become dynamical variables. We also introduce their conjugate momenta p_0 and π_a , respectively. Define $Q^I \equiv (q^\mu, \lambda^a)$ and $P_I \equiv (p_\mu, \pi_a)$, for $I = 0, \dots, n + m$. We can view this as a sequence of embeddings,

$$\mathcal{Q}^{n-m} \hookrightarrow \mathcal{M}^n \hookrightarrow \widehat{\mathcal{M}}^{n+m+1}, \quad (2.4)$$

where $\widehat{\mathcal{M}}^{n+m+1} \equiv \mathcal{M}^n \times \mathbb{R}^m \times \mathbb{R}$. The associated cotangent bundle $T^*\widehat{\mathcal{M}}$ has dimension $2(n + m + 1)$ and local coordinates (Q^I, P_I) . On this *extended phase space*, we can define a generic Hamiltonian $\mathcal{H}(\mathbf{Q}, \mathbf{P})$ with standard Hamilton's equations,

$$\frac{dQ^I}{ds} = \frac{\partial \mathcal{H}}{\partial P_I}, \quad \frac{dP_I}{ds} = -\frac{\partial \mathcal{H}}{\partial Q^I}. \quad (2.5)$$

This system is conservative, $d\mathcal{H}/ds = 0$, since \mathcal{H} does not depend explicitly on time—we denote the “new” time parametrization by s . Now, suppose we choose this Hamiltonian to have the form

$$\mathcal{H}(\mathbf{Q}, \mathbf{P}) \equiv H_{\text{total}}(q^0, \mathbf{q}, \boldsymbol{\lambda}, \mathbf{p}) + p_0. \quad (2.6)$$

The equations of motion (2.5) then become (see Fig. 1 for an illustration of the symplectification procedure)

$$\frac{dq^0}{ds} = 1, \quad (2.7a)$$

$$\frac{dp_0}{ds} = -\frac{\partial H}{\partial q^0} - \lambda^a \frac{\partial \psi_a}{\partial q^0}, \quad (2.7b)$$

$$\frac{dq^i}{ds} = \frac{\partial H}{\partial p_i} + \lambda^a \frac{\partial \psi_a}{\partial p_i}, \quad (2.7c)$$

$$\frac{dp_i}{ds} = -\frac{\partial H}{\partial q_i} - \lambda^a \frac{\partial \psi_a}{\partial q^i}, \quad (2.7d)$$

$$\frac{d\lambda^a}{ds} = 0, \quad (2.7e)$$

$$\frac{d\pi_a}{ds} = -\psi_a. \quad (2.7f)$$

We can enforce the constraints by setting $\pi_a = 0$, so that Eq. (2.7f) becomes $\psi_a(q^0, \mathbf{q}, \mathbf{p}) = 0$. Eq. (2.7e) simply says that the Lagrange multipliers do not change on the constraint surface. Eq. (2.7a) yields $q^0 = t = s$ (by setting the integration constant to zero). Eq. (2.7b) becomes $dp_0/dt = -\partial H_{\text{total}}/\partial t = dH_{\text{total}}/dt$, i.e., $p_0(t) = -H_{\text{total}}(t) \approx -H(t)$, up to a constant that can be chosen to be zero. Thus, p_0 is simply the value of the original Hamiltonian on the

constraint surface. Finally, Eqs. (2.7c) and (2.7d) yield the original equations of motion (2.2). Therefore, we have embedded the degrees of freedom of system (2.2) into the phase space of a higher dimensional *conservative* Hamiltonian system (2.5). The original nonconservative and constrained system is recovered from (2.6) under the “gauge fixing”

$$\pi_a = 0, \quad s = q^0 = t, \quad p_0(t) = -H_{\text{total}}(t) \approx -H(t). \quad (2.8)$$

The phase space of the original system lives on a hypersurface $\partial\mathcal{S}$ embedded into $T^*\widehat{\mathcal{M}}$, defined by

$$\mathcal{H}|_{\partial\mathcal{S}} \approx H(q^0, \mathbf{q}, \mathbf{p}) + p_0 \approx 0. \quad (2.9)$$

Definition 1 (See [11]). A smooth manifold of dimension $2n$ endowed with a closed and nondegenerate 2-form Ω is called a *symplectic manifold*, and Ω is called a *symplectic form*. A smooth manifold of dimension $2n + \bar{n}$, $\bar{n} > 0$, endowed with a closed 2-form ω of rank $2n$ that is degenerate is called a *presymplectic manifold*, and ω is called a *presymplectic form*.

The Hamiltonian system (2.5) has a closed and nondegenerate symplectic 2-form given by

$$\Omega \equiv dQ^I \wedge dP_I = dq^0 \wedge p_0 + dq^i \wedge dp_i + d\lambda^a \wedge d\pi_a, \quad (2.10)$$

which is preserved, i.e., the Lie derivative along the flow vanishes, $\mathcal{L}_{\mathcal{H}}\Omega = 0$. Thus, $(T^*\widehat{\mathcal{M}}, \Omega)$ is a *symplectic manifold*. However, under the gauge fixing (2.8), we recover the nonconservative and constrained system (2.2) with a *restricted presymplectic* 2-form

$$\omega \equiv \Omega|_{\partial\mathcal{S}} = dq^i \wedge dp_i, \quad (2.11)$$

which has rank $2n$ over a space of dimension $2n+2m+2$. It therefore follows that ω is degenerate, and the phase space $(T^*\mathcal{Q}, \omega)$ of system (2.2) is a *presymplectic manifold*. For conservative and constrained Hamiltonian systems such a presymplectic structure has already been noted [25], as well as for dissipative but unconstrained cases [24]. The above discussion incorporates both situations. We say that system (2.2) admits a *symplectification* since its phase space can be recovered by a restriction of a higher dimensional symplectic phase space.

2.3 Presymplectic integrators

As we have seen, a conservative Hamiltonian system (2.5) has a symplectic form Ω that is constant. Let $\Phi_h : T^*\widehat{\mathcal{M}} \rightarrow T^*\widehat{\mathcal{M}}$ be a *symplectic integrator* for system (2.5), where $h > 0$ is the discretization step size such that $s_\ell = h\ell$, for iterations $\ell = 0, 1, \dots$ (s denotes time). A symplectic integrator is by definition a discretization that exactly preserves the symplectic form [19–23], i.e., $\Omega(s_\ell) = \Phi_h^\ell \circ \Omega(0) = \Omega(0)$, where Φ_h^ℓ denotes ℓ iterations of the map Φ_h . The numerical integrator is said to be of order $r > 1$ if the global error in approximating the continuous-time trajectory is $\mathcal{O}(h^r)$ [23].

Theorem 2 (See [24]). *A dynamical system with phase space $T^*\widehat{\mathcal{M}}$ preserves the symplectic form Ω if and only if it is (locally) a conservative Hamiltonian system (2.5).*

As a consequence, a symplectic integrator admits a (local) Hamiltonian which is a perturbation in terms of the step size, $\widetilde{\mathcal{H}} = \mathcal{H} + h^r \Delta\mathcal{H}_1 + \dots$, called *shadow Hamiltonian* [19]. This allows one to study the numerical method purely from a continuum analysis. The existence of a shadow Hamiltonian is key in explaining the success of symplectic integrators. (Other types of integrators that are not symplectic do not admit a shadow Hamiltonian.) We now introduce a similar notion to symplectic integrators but for nonconservative and constrained systems.

Definition 3. A numerical map $\phi_h : T^*\mathcal{Q} \rightarrow T^*\mathcal{Q}$ is said to be a *presymplectic integrator* to the nonconservative and constrained Hamiltonian system (2.2) if it is obtained by a reduction, i.e., by the gauge fixing (2.8), of a symplectic integrator Φ_h for its symplectification, namely system (2.5)/(2.6).

Thus, presymplectic integrators are essentially constructed from symplectic integrators. The crucial difference is that they preserve the presymplectic form ω , which is no longer constant. Given a conservative Hamiltonian, obtained from a non-singular Lagrangian, one can construct the exact discrete Lagrangian which solves the Hamilton-Jacobi equation [26]. Integrators obtained from a discrete Lagrangian are symplectic and admit a *globally* defined shadow Hamiltonian. Such integrators are called *variational integrators*.

Assumption 4. We assume the base symplectic integrator Φ_h is a variational integrator [26].

With these ingredients, we state our next result that extends one of the main results of [24] to arbitrary smooth manifolds \mathcal{M} and for constrained cases.

Theorem 5. *Let ϕ_h be a presymplectic integrator of order r for the nonconservative and constrained Hamiltonian system (2.2), whose true flow is denoted by φ_t . Then this method preserves the time-varying Hamiltonian up to a bounded error,*

$$H \circ \phi_h^\ell = H \circ \varphi_{t_\ell} + \mathcal{O}(h^r), \quad (2.12)$$

where $t_\ell = h\ell = \mathcal{O}(h^r e^{c/h})$ is the simulation time, with some constant $c > 0$, and $\ell = 0, 1, \dots$. Moreover, the method admits a shadow Hamiltonian $\tilde{H} = H + h^r \Delta H_r + \dots$ that is globally defined.

Proof sketch. The basic idea involves using the symplectification (2.6), allowing us to rely on standard results for symplectic integrators ensuring $\mathcal{H} \circ \Phi_h^\ell = \mathcal{H} \circ \widehat{\varphi}_{s_\ell} + \mathcal{O}(h^r)$, where Φ_h is the base variational integrator and $\widehat{\varphi}_{s_\ell}$ is the true flow of (2.6). We then apply the gauge fixing (2.8) on the numerical map to obtain (2.12). The shadow Hamiltonian for ϕ_h follows under Assumption 4. ■

3 Dissipative Geodesic under Constraints

Consider the total Hamiltonian

$$H_{\text{total}} = \frac{1}{2} e^{-\eta(t)} g^{ij}(\mathbf{q}) p_i p_j + e^{\eta(t)} f(\mathbf{q}) + e^{\eta(t)} \lambda^a \psi_a(\mathbf{q}), \quad (3.1)$$

where $\eta(t) > 0$ is a generic dissipation function, and g_{ij} is the Riemannian metric of \mathcal{M} . Note that we choose the constraints in (2.1) to have the factorized form $\psi_a(t, \mathbf{q}, \mathbf{p}) \mapsto e^{\eta(t)} \psi_a(\mathbf{q})$, and now ψ_a depends only on the position (holonomic). Hamilton's equations for (3.1) can be reduced to

$$\ddot{q}^i + \Gamma^i_{jk} \dot{q}^j \dot{q}^k + \dot{\eta}(t) \dot{q}^i \approx -g^{ij} \partial_j f - g^{ij} \lambda^a \partial_j \psi_a, \quad (3.2)$$

where Γ^i_{jk} are the Christoffel symbols. This is a *dissipative geodesic equation* subject to constraints $\psi(\mathbf{q}) = \mathbf{0}$ —note that if $\dot{\eta} = 0$, $f = 0$ and $\psi_a = 0$ we recover a standard geodesic over \mathcal{M} . Suppose that for such a general system one is able to prove a rate of convergence. Then a presymplectic integrator closely reproduces this rate as follows.

Corollary 6. Consider system (3.2) over a Riemannian manifold \mathcal{M} and subject to constraints. Let ϕ_h be a presymplectic integrator of order r (Definition 3). Assume this numerical integrator has a Lipschitz constant $L_\phi > 0$. Then such an integrator preserves the convergence rates in the sense that

$$\underbrace{f \circ \phi_h^\ell - \min f}_{\text{discrete-time rate}} = \underbrace{f \circ \varphi_{t_\ell} - \min f}_{\text{continuous-time rate}} + \underbrace{\mathcal{O}(h^r e^{-\eta(t_\ell)})}_{\text{small error}}, \quad (3.3)$$

provided $e^{L_\phi - \eta(t_\ell)} < \infty$ and $t_\ell = \mathcal{O}(h^r e^{c/h})$ for some constant $c > 0$.

Proof sketch. The result is an immediate consequence of Eq. (2.12) together with the Lipschitz condition for the numerical map (which is standard). ■

This result shows that presymplectic integrators are able to closely preserve the continuous-time rates of convergence in general. The error term can be exponentially small, thus negligible in practice, and the simulation time exponentially large, not incurring practical limitations. Next, we show some stability analysis results for system (3.2).

Theorem 7. The pair $(\mathbf{q}_\star, \boldsymbol{\lambda}_\star)$ is a critical point of system (3.2) only if it satisfies the KKT conditions for the optimization problem

$$\min_{\mathbf{q} \in \mathcal{M}} f(\mathbf{q}) \quad \text{s.t.} \quad \boldsymbol{\psi}(\mathbf{q}) = \mathbf{0}, \quad (3.4)$$

namely

$$\partial_i f(\mathbf{q}_\star) + \lambda_\star^a \partial_i \psi_a(\mathbf{q}_\star) = 0, \quad \psi_a(\mathbf{q}_\star) = 0, \quad (3.5)$$

for $i = 1, \dots, n$ and $a = 1, \dots, m$.

Proof sketch. This follows immediately by writing Eq. (3.2) in first order form. ■

Theorem 8. The system (3.2) is stable around an isolated minimizer of problem (3.4). In addition, if the damping is constant, $\eta(t) = \gamma t$ with $\gamma = \text{const.} > 0$, then the system is asymptotically stable.

Proof sketch. This is obtained by considering the Lyapunov function $\mathcal{E} = (1/2)g^{ij}(\mathbf{q})p_i p_j + f(\mathbf{q}) + \lambda^a \psi_a(\mathbf{q})$, which is the mechanical energy, and showing that $\dot{\mathcal{E}} \leq 0$. When the damping is constant, asymptotic stability follows from LaSalle's invariance principle. ■

These last two results show that system (3.2) is able to solve problem (3.4) under suitable conditions. We are also interested in knowing how fast it converges to the solution. We provide a local result.

Theorem 9. In a sufficiently small neighborhood of an isolated minimizer \mathbf{q}_\star of problem (3.4), the system (3.2) with a constant damping $\eta = \gamma t$ such that $\gamma \leq 2\sqrt{\omega_{\min}}$, and initial conditions $\mathbf{q}_0 \equiv \mathbf{q}(0)$ and $\dot{\mathbf{q}}(0) = \mathbf{0}$ obeying the constraints, has a convergence rate of

$$\|\mathbf{q}(t) - \mathbf{q}_\star\|^2 \leq e^{-2\sqrt{\omega_{\min}}t} \|\mathbf{q}_0 - \mathbf{q}_\star\|^2, \quad (3.6)$$

where $\omega_{\min} > 0$ is the smallest eigenvalue of the projected Hessian $(g^{-1}\mathcal{P}\nabla^2 f \mathcal{P}^T g^{-1})|_{\mathbf{q}_\star}$ at the critical point, where \mathcal{P} is the projection operator to the constraint surface defined in Eq. (5.3).

This result implies that that one can obtain discretizations able to achieve *optimal rates* locally. To see this, suppose we have a discretization with step size $h > 0$, $t_\ell = h\ell$, for iterations $\ell = 0, 1, \dots$. Restoring a mass m into (3.2) (see Eq. (B.7) in the Appendix) the rate (3.6) changes to $e^{-2\sqrt{\omega_{\min}/mt}}$. Choosing $m = h$, step size

$$h = C^2/\omega_{\max}, \quad (3.7)$$

where ω_{\max} is the largest eigenvalue of the projected Hessian from Theorem 9, and C is related to the numerical stability of the integrator, the rate (3.6) becomes

$$\|\mathbf{q}_\ell - \mathbf{q}_\star\|^2 \leq e^{-2C\sqrt{Q^{-1}}\ell} \|\mathbf{q}_0 - \mathbf{q}_\star\|^2, \quad (3.8)$$

provided the error in the discretization can be neglected compared to this rate—which is the case for presymplectic integrators according to Eq. (3.3). Above, $Q \equiv \omega_{\max}/\omega_{\min}$ is the *condition number* of the problem. Interestingly, for the presymplectic integrator we introduce in the next section, $C = 2$, in which case the rate (3.8) achieves precisely the well-known lower bound (optimal rate) for smooth, strongly convex, but *unconstrained* problems on \mathbb{R}^n , namely [27]

$$\|\mathbf{q}_\ell - \mathbf{q}_\star\|^2 \geq \left(\frac{\sqrt{Q} - 1}{\sqrt{Q} + 1}\right)^{2\ell} \|\mathbf{q}_0 - \mathbf{q}_\star\|^2 \simeq e^{-4\sqrt{Q^{-1}}\ell} \|\mathbf{q}_0 - \mathbf{q}_\star\|^2. \quad (3.9)$$

Thus, suitable discretizations of system (3.2) are able to achieve this optimal/accelerated lower bound at least locally (or get very close to it depending on C), and on more general settings than previously considered.

4 General KKT Conditions on Manifolds

Consider adding inequality constraints to problem (3.4),

$$\min_{\mathbf{q} \in \mathcal{M}} f(\mathbf{q}) \quad \text{s.t.} \quad \boldsymbol{\psi}(\mathbf{q}) = \mathbf{0}, \quad \boldsymbol{\phi}(\mathbf{q}) \leq \mathbf{0}, \quad (4.1)$$

where $\boldsymbol{\phi} = (\phi_1, \dots, \phi_{\bar{m}})$. Inside the feasible region, inequality constraints are *inactive*. They only play a role and become *active* on the boundary of the region. Effectively, inequality constraints thus behave as equality constraints but they can be switched “on/off.” Let us first focus on a single inequality constraint ϕ_b ($b = 1, \dots, \bar{m}$) with associated Lagrange multiplier μ^b . We have either $\phi_b(\mathbf{q}) < 0$, in which case we can set $\mu^b = 0$ since the constraint is inactive, or $\phi_b(\mathbf{q}) = 0$, in which case $\mu^b \neq 0$. We thus have (with no summation over b implied)

$$\mu^b \cdot \phi_b(\mathbf{q}) = 0. \quad (4.2)$$

Geometrically, the constraint is active if it “pulls” in the opposite of f ’s descent direction, i.e., $(-\partial_i f)(-\partial^i \phi_b) \leq 0$. Thus, at a given point \mathbf{q} , if $\partial_i f \partial^i \phi_b \leq 0$ then the constraint ϕ_b is active, and otherwise it is inactive. A critical point must obey $\partial_j f(\mathbf{q}_\star) + \mu_\star^c \partial_j \phi_c(\mathbf{q}_\star) = 0$, for $c = 1, \dots, \bar{m}$. Contracting this last expression with $\partial_i \phi_b(\mathbf{q}_\star)$ we conclude that

$$\mu_\star^c \partial_i \phi_b(\mathbf{q}_\star) \partial^i \phi_c(\mathbf{q}_\star) \geq 0, \quad (4.3)$$

where we used $\mu_\star^c = 0$ for inactive constraints. Noticing that $\partial_i \phi_b \partial^i \phi_c = (\partial_{\mathbf{q}} \boldsymbol{\phi} \partial_{\mathbf{q}} \boldsymbol{\phi}^T)_{bc}$ are entries of a positive semidefinite matrix, this relation implies that

$$\mu_\star^b \geq 0 \quad (b = 1, \dots, \bar{m}). \quad (4.4)$$

Now, consider the Hamiltonian system

$$H_{\text{total}} = \frac{1}{2}e^{-\eta(t)}g^{ij}(\mathbf{q})p_i p_j + e^{\eta(t)}f(\mathbf{q}) + e^{\eta(t)}\lambda^a\psi_a(\mathbf{q}) + e^{\eta(t)}\mu^b\phi_b(\mathbf{q}), \quad (4.5)$$

which yield the equations of motion

$$\ddot{q}^i + \Gamma^i_{jk}(\mathbf{q})\dot{q}^j\dot{q}^k + \dot{\eta}(t)\dot{q}^i = -g^{ij}(\mathbf{q}) \left[\partial_j f(\mathbf{q}) + \lambda^a \partial_j \psi_a(\mathbf{q}) + \mu^b \partial_j \phi_b(\mathbf{q}) \right], \quad (4.6a)$$

$$0 = \psi_a(\mathbf{q}) \quad (a = 1, \dots, m), \quad (4.6b)$$

$$0 \geq \phi_b(\mathbf{q}) \quad (b = 1, \dots, \bar{m}). \quad (4.6c)$$

Importantly, it is implicit that $\mu^b(t) = 0$ whenever $\phi_b(\mathbf{q}(t)) < 0$ (inactive), so that the system becomes unconstrained with respect to ϕ_b in such case. Therefore, Eq. (4.2) is always satisfied during the evolution of the system. The condition (4.6c) is effectively an equality, in the same way as (4.6b). The argument used in obtaining condition (4.3) at stationarity is still valid, which implies (4.4). We thus have:

- Critical points of system (4.6) obey the KKT conditions (see Theorem 10 in the Appendix)

$$\partial_j f(\mathbf{q}_\star) + \lambda_\star^a \partial_j \psi_a(\mathbf{q}_\star) + \mu_\star^b \partial_j \phi_b(\mathbf{q}_\star) = 0, \quad (4.7a)$$

$$\psi_a(\mathbf{q}_\star) = 0, \quad \phi_b(\mathbf{q}_\star) \leq 0, \quad (4.7b)$$

$$\mu_\star^b \cdot \phi_b(\mathbf{q}_\star) = 0, \quad (4.7c)$$

$$\mu_\star^b \geq 0. \quad (4.7d)$$

- Theorems 8 and 9 also remain true in this case. The reason is because an inequality constraint ϕ_b only participates in the dynamics when it is active, but then it behaves as an equality constraint, $\phi_b(\mathbf{q}) = 0$ when $\mu^b \neq 0$ (see the Appendix for details).

5 Dissipative RATTLE for Constrained Optimization

The system (4.6) is very general as it incorporates constraints over an arbitrary Riemannian manifold \mathcal{M} . A numerical simulation requires computing Γ^i_{jk} , which involves derivatives of the metric g_{ij} . Recalling the discussion in the introduction, it is convenient to use an embedding into $\mathcal{M} \equiv \mathbb{R}^n$, where g_{ij} can be taken globally as *constant*, so that $\Gamma^i_{jk} = 0$. This simplifies the construction of geometric integrators, resulting in simple and explicit updates. Thus, here we focus on this case and propose a presymplectic integrator for solving the problem

$$\min_{\mathbf{q} \in \mathbb{R}^n} f(\mathbf{q}) \quad \text{s.t.} \quad \boldsymbol{\psi}(\mathbf{q}) = \mathbf{0}, \quad \boldsymbol{\phi}(\mathbf{q}) \leq \mathbf{0}. \quad (5.1)$$

This is done by simulating (4.6) with $\Gamma^i_{jk} = 0$ and $\eta(t) = \gamma t$, $\gamma = \text{const.} > 0$. Following Definition 3, we derive a presymplectic integrator of order $r = 2$ based on a modern reformulation of the famous RATTLE integrator [28–31], widely used in molecular dynamics. The derivation is long but straightforward, and involves a few technical tricks that are fully described in the Appendix.

To incorporate both equality and inequality constraints, define the augmented vector of constraints $\boldsymbol{\Psi} \equiv (\psi_1, \dots, \psi_m; \phi_1, \dots, \phi_{\bar{m}})$, and Lagrange multipliers $\boldsymbol{\Lambda} \equiv (\lambda_1, \dots, \lambda_m; \mu_1, \dots, \mu_{\bar{m}})$. Let $\mathcal{J}(\mathbf{q})$ denote the $(m + \bar{m}) \times n$ Jacobian matrix of constraints at point \mathbf{q} , defined as

$$\mathcal{J}_{ai}(\mathbf{q}) \equiv \begin{cases} \partial \Psi_a / \partial q^i |_{\mathbf{q}} & \text{if } \Psi_a(\mathbf{q}) \text{ is active,} \\ 0 & \text{if } \Psi_a(\mathbf{q}) \text{ is inactive,} \end{cases} \quad (5.2)$$

Algorithm 1 DISSRATTLE is a presymplectic integrator for problem (5.1). The algorithm has one parameter $\alpha \in (0, 1)$ (momentum factor) and step size $h > 0$. The parameter $\beta = \cosh(-\log \alpha)$ is fixed, and $g \succ 0$ is an arbitrary symmetric matrix (preconditioner).

```

1: for  $\ell = 0, 1, \dots$  do
2:    $\mathbf{p}_{\ell+1/2} \leftarrow \alpha \mathcal{P}(\mathbf{q}_\ell) [\mathbf{p}_\ell - (h/2) \nabla f(\mathbf{q}_\ell)]$ 
3:    $\tilde{\mathbf{p}}_{\ell+1/2} \leftarrow \mathbf{p}_{\ell+1/2} - (h\alpha/2) \mathcal{J}(\mathbf{q}_\ell)^T \mathbf{\Lambda}_\ell$ 
4:    $\mathbf{q}_{\ell+1} \leftarrow \mathbf{q}_\ell + \beta g^{-1} \tilde{\mathbf{p}}_{\ell+1/2}$ 
5:   for  $a = 1, \dots, m + \bar{m}$  do
6:     if  $\Psi_a$  is active then
7:        $\Lambda_{a,\ell} \leftarrow \Psi_a(\mathbf{q}_{\ell+1}) = 0$ 
8:     else
9:        $\Lambda_{a,\ell} \leftarrow 0$ 
10:    end if
11:  end for
12:   $\mathbf{p}_{\ell+1} \leftarrow \mathcal{P}(\mathbf{q}_{\ell+1}) [\alpha \tilde{\mathbf{p}}_{\ell+1/2} - (h/2) \nabla f(\mathbf{q}_{\ell+1})]$ 
13: end for

```

where $i = 1, \dots, n$ and $a = 1, \dots, m + \bar{m}$. Equality constraints, $\Psi_a = \psi_a$, are always active. Inequality constraints, $\Psi_a = \phi_a$, must be checked point-wise. Define also the projection operators

$$\mathcal{R}(\mathbf{q}) \equiv \mathcal{J}(\mathbf{q})g^{-1}\mathcal{J}(\mathbf{q})^T, \quad \mathcal{P}(\mathbf{q}) \equiv I - \mathcal{J}(\mathbf{q})^T\mathcal{R}(\mathbf{q})^{-1}\mathcal{J}(\mathbf{q})g^{-1}. \quad (5.3)$$

With these ingredients, we state Algorithm 1.

The parameter $\alpha \in (0, 1)$ is related to the damping γ . Increasing α corresponds to decreasing γ , i.e., $\alpha \rightarrow 1$ corresponds to $\gamma \rightarrow 0$, and $\alpha \rightarrow 0$ to $\gamma \rightarrow \infty$. The parameter $\beta \equiv \cosh(-\log \alpha)$ is fixed. The updates 2–11 must be solved simultaneously, with the components of $\mathbf{\Lambda}_\ell$ determined by solutions to the algebraic equations in step 7 when the constraint Ψ_a is active, and otherwise the Lagrange multiplier is set to zero. We wrote component-wise but in practice these updates can be computed vectorially with the aid of any root finding routine (when a closed form solution is unavailable). This algorithm requires only one gradient computation of f per iteration (the last one can be reused in the subsequent iteration). Finally, instead of a constant α one is free to use an adaptive α_ℓ , which would be associated to a time-dependent damping $\gamma \mapsto \gamma(t)$. Conveniently, this method uses the Euclidean gradient ∇f instead of parallel transports or geodesic flows, i.e., approximations to the exponential map. Note also that there is freedom to choose a constant positive definite and symmetric metric g that acts as a *preconditioner*, which can further improve convergence. Algorithm 1 is of order $r = 2$ and obeys Corollary 6.

6 Numerical Example

We consider an important model in the theory of disordered systems, the spherical Sherrington-Kirkpatrick (SSK) model, which provides a baseline for random optimization problems. We follow the setup of [32]. The system is described by a Hamiltonian (energy)

$$\mathcal{H}(\boldsymbol{\sigma}) = -\frac{1}{2}\boldsymbol{\sigma}^T M \boldsymbol{\sigma} - \rho \mathbf{g}^T \boldsymbol{\sigma}, \quad (6.1)$$

where $\boldsymbol{\sigma} \in \mathcal{S}_{n-1}$ lies on the hypersphere of radius $\|\boldsymbol{\sigma}\| = \sqrt{n}$ —note that $\boldsymbol{\sigma}$ plays the role of \mathbf{q} in our previous notation. The disorder matrix M is symmetric with i.i.d. entries $M_{ij} \sim$

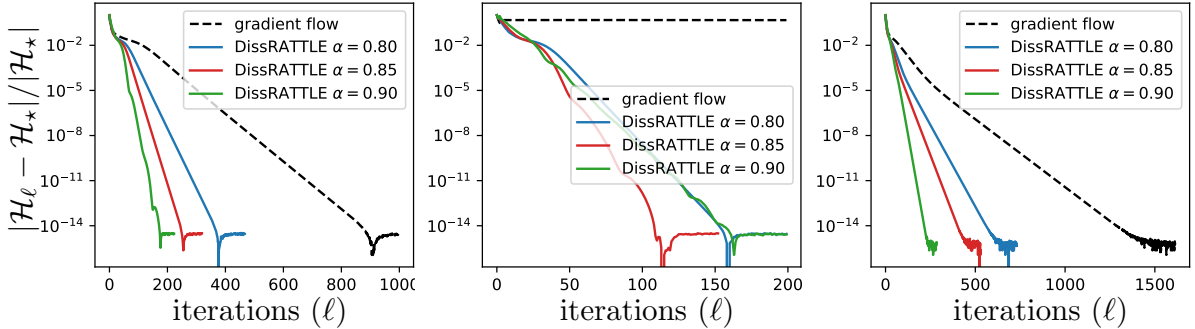


Figure 2: Solving problem (6.1)/(6.2) with Algorithm 1 and Riemannian gradient descent. We set $n = 1000$ dimensions. *Left:* Step size $h = 0.9/\lambda_{\max}(M)$ for both methods, and no external field ($\rho = 0$). *Middle:* Same problem but increased step size, $h = 1.9/\lambda_{\max}(M)$. *Right:* We add an external field ($\rho = 0.1$). We set $h = 0.9/\lambda_{\max}(M)$ for both methods.

$\mathcal{N}(0, (1 + \delta_{ij})/n)$, where δ_{ij} is the Kronecker delta. The external field \mathbf{g} has i.i.d. entries from a standard Gaussian, $\mathcal{N}(0, 1)$. The goal is to solve

$$\min_{\sigma \in \mathcal{S}_{n-1}} \mathcal{H}(\sigma). \quad (6.2)$$

We compare Algorithm 1 with Riemannian gradient descent [7], here denoted as “gradient flow.” In the absence of external field, $\rho = 0$, it can be shown that the problem has an exact solution, $\mathcal{H}_* = -\frac{n}{2}\lambda_{\max}(M)$. When $\rho \neq 0$ the problem does not have a closed form solution, thus we set \mathcal{H}_* the smallest value obtained when $\ell \rightarrow \infty$. In Fig. 2 we show one instance of this problem. For all methods, we choose the largest step size $h = 0.9/\lambda_{\max}(M)$ allowed by gradient flow to converge (left and right plots). Algorithm 1 is *significantly faster and much more stable*, allowing even larger step sizes (middle plot). We pick three different values of α for illustration. The parameter α was not tuned at all, and if one carefully tune h and α , Algorithm 1 is even faster than illustrated in these plots. Details about the implementation as well additional experiments are provided in the Appendix.

7 Conclusion

We introduced a general framework for constructing optimization methods over smooth manifolds and for problems with nonlinear (equality/inequality) constraints. Our approach relies on a dissipative extension of Dirac’s formalism of constrained Hamiltonian systems. As a result, we derived a dissipative geodesic equation that is consistent with the KKT conditions on Riemannian manifolds. Such a system was shown to have favorable stability and convergence rate properties.

We also extended symplectic integrators to dissipative and constrained cases over manifolds. Such discretizations preserve the main properties of the continuum dynamics, and in particular its convergence rates (up to a controlled error). Based on these ideas, we derived a simple and efficient method based on a dissipative extension of the famous RATTLE integrator. Such a method is able to solve optimization problems with equality and inequality constraints. Numerically, this method proved to be highly stable and fast.

We deferred many technical details and additional results to the Appendix, such as the proofs of the main results, and a method for optimization over Lie groups.

Finally, this work lays out the foundations of a general approach to constrained optimization on manifolds. There are many possible extensions and refinements of our results. For instance, it would be interesting to obtain more general (global) convergence rate results for systems (3.2) or (4.6), based on Theorem 11 in the Appendix.

Acknowledgements

This work is supported by the Army Research Office (ARO) under contract W911NF-17-1-0304 as part of the collaboration between US DOD, UK MOD and UK Engineering and Physical Research Council (EPSRC) under the Multidisciplinary University Research Initiative (MURI).

A Review of Conservative Hamiltonian Systems

In this section, we provide a brief review of the geometric formulation of conservative Hamiltonian systems. The goal is to recall basic concepts and introduce notation; we refer to [11, 33, 34] for details. This paper assumes familiarity with differential geometry and tensor manipulations as commonly found in general relativity [35, 36].

Given a smooth n -dimensional manifold \mathcal{M} , we can construct its cotangent bundle $T^*\mathcal{M}$, which is the union of all cotangent spaces $T_{\mathbf{p}}^*\mathcal{M}$ for all points $\mathbf{p} \in \mathcal{M}$.¹ The cotangent bundle carries a canonical symplectic structure ω that will be defined shortly. Around any point $\mathbf{p} \in \mathcal{M}$ there exists local coordinates $\mathbf{q} = (q^1, \dots, q^n)$ on \mathbb{R}^n . We henceforth refer to \mathbf{p} simply by its coordinates \mathbf{q} when clear from the context. The cotangent bundle then inherits local coordinates (q^i, p_i) , for $i = 1, \dots, n$, around $T_{\mathbf{q}}^*\mathcal{M}$ (p_i denotes the momentum, which is the dual to q^i). Thus, $T_{\mathbf{q}}^*\mathcal{M}$ can be locally identified with \mathbb{R}^{2n} . In such a coordinate basis we can write the symplectic 2-form²

$$\omega \equiv dq^i \wedge dp_i, \quad (\text{A.1})$$

where \wedge denotes the exterior or wedge product between differential forms [11]. This 2-form is nondegenerate since its rank is $2n$, and also closed, $d\omega = 0$ (d is the exterior derivative), hence $(T^*\mathcal{M}, \omega)$ is a *symplectic manifold* [11]. This is always true, namely for any smooth manifold \mathcal{M} . Therefore, the cotangent bundle $T^*\mathcal{M}$ of any smooth manifold \mathcal{M} is a symplectic manifold.

Given a function $H : T^*\mathcal{M} \rightarrow \mathbb{R}$, called Hamiltonian, the 2-form ω induces a dynamical system obeying Hamilton's equations,

$$\dot{q}^i = \frac{\partial H}{\partial p_i}, \quad \dot{p}_i = -\frac{\partial H}{\partial q^i}, \quad (\text{A.2})$$

for $i = 1, \dots, n$, where $\dot{q}^i \equiv dq^i/dt$ and t denotes time parametrization. It is immediate that

$$\frac{dH}{dt} = 0, \quad (\text{A.3})$$

i.e., H is conserved. Hamilton's equations (A.2) can be more concisely written as

$$i_{X_H}(\omega) = -dH, \quad (\text{A.4})$$

¹The cotangent space $T_{\mathbf{p}}^*\mathcal{M}$ is the dual vector space to the tangent space $T_{\mathbf{p}}\mathcal{M}$. It exists independently of $T_{\mathbf{p}}\mathcal{M}$ and cannot be identified with it without further structure, such as a Riemannian metric.

²We use Einstein's summation where repeated upper and lower indices are summed over, i.e., $u^i v_i \equiv \sum_i u^i v_i$. Also, upper indices, u^i , denote components of vectors, $\mathbf{u} \in T\mathcal{M}$, whereas lower indices, v_i , denote components of covectors (or dual vectors), $\mathbf{v} \in T^*\mathcal{M}$.

where i_{X_H} is the interior product and X_H is the Hamiltonian vector field, given by

$$X_H \equiv \dot{q}^i \frac{\partial}{\partial q^i} + \dot{p}_i \frac{\partial}{\partial p_i}. \quad (\text{A.5})$$

From (A.4), together with Cartan's formula, one can easily show that the symplectic structure is preserved, namely $\mathcal{L}_{X_H}\omega = 0$, where \mathcal{L}_{X_H} is the Lie derivative along the vector field X_H . Conversely, one can show that any vector field X that preserves ω must, locally, obey Eq. (A.4) for some function H , i.e., X must be, at least locally, the vector field of a Hamiltonian system ($X = X_H$). This is the reason why Hamiltonian systems are special: They are the only dynamics that preserve the canonical symplectic structure of the cotangent bundle $T^*\mathcal{M}$ of any smooth manifold \mathcal{M} ; this is essentially the proof of Theorem 2.

Symplectic integrators

This special class of numerical integrators consists of discretizations of conservative Hamiltonian systems required to exactly preserve the symplectic structure ω [21, 23]. Therefore, such discretizations can be seen as Hamiltonian systems themselves, with a perturbed or *shadow Hamiltonian* that is a formal expansion around the true Hamiltonian of the system in terms of the step size. In short, such a class of numerical integrators inherits all the benefits of being Hamiltonian.

B The Dissipative Constrained Geodesic Equation

Here we derive the geodesic equation (3.2). Consider the Hamiltonian (3.1) but with an additional mass term, i.e.,

$$H_{\text{total}} = \frac{1}{2m} e^{-\eta} g^{ij} p_i p_j + e^\eta f + e^\eta \lambda^a \psi_a. \quad (\text{B.1})$$

Hamilton's equations yield

$$\dot{q}^i \approx \frac{\partial H_{\text{total}}}{\partial p_i} = \frac{1}{m} e^{-\eta} g^{ij} p_j, \quad (\text{B.2a})$$

$$\dot{p}_i \approx -\frac{\partial H_{\text{total}}}{\partial q^i} = -\frac{1}{2m} e^{-\eta} \partial_i g^{jk} p_j p_k - e^\eta \partial_i f - e^\eta \lambda^a \partial_i \psi_a. \quad (\text{B.2b})$$

These equations are subject to the constraints $\psi_a(\mathbf{q}) = 0$, hence the symbol \approx according to Dirac's notation. Differentiating the first equation with respect to time,

$$\ddot{q}^i \approx \frac{1}{m} e^{-\eta} g^{ij} \dot{p}_j + \frac{1}{m} e^{-\eta} \partial_k g^{ij} \dot{q}^k p_j - \frac{1}{m} \dot{\eta} e^{-\eta} g^{ij} p_j. \quad (\text{B.3})$$

Replacing (B.2b),

$$\ddot{q}^i \approx \frac{1}{m} e^{-\eta} \partial_k g^{ij} \dot{q}^k p_j - \frac{1}{m} \dot{\eta} e^{-\eta} g^{ij} p_j - \frac{1}{2m^2} e^{-2\eta} g^{ij} \partial_j g^{kl} p_k p_l - \frac{1}{m} g^{ij} \partial_j f - \frac{1}{m} \lambda^a g^{ij} \partial_j \psi_a. \quad (\text{B.4})$$

From (B.2a) we have $p_i = m e^\eta g_{ij} \dot{q}^j$, which replaced above yields

$$\ddot{q}^i - g_{j\ell} \partial_k g^{ij} \dot{q}^k \dot{q}^\ell + \frac{1}{2} g^{ij} \partial_j g_{k\ell} \dot{q}^k \dot{q}^\ell + \dot{\eta} \dot{q}^i \approx -\frac{1}{m} g^{ij} \partial_j f - \frac{1}{m} \lambda^a g^{ij} \partial_j \psi_a. \quad (\text{B.5})$$

Using $g_{j\ell} \partial_k g^{ij} = -g^{ij} \partial_k g_{j\ell}$ and the definition of Christoffel symbols,

$$\Gamma_{ijk} \equiv \frac{1}{2} (\partial_k g_{ij} + \partial_j g_{ik} - \partial_i g_{jk}), \quad \Gamma^i_{jk} \equiv g^{im} \Gamma_{mjk}, \quad (\text{B.6})$$

this last equation can be written as

$$\ddot{q}^i + \Gamma^i_{jk} \dot{q}^j \dot{q}^k + \dot{\eta} \dot{q}^i \approx -\frac{1}{m} g^{ij} (\partial_j f + \lambda^a \partial_j \psi_a). \quad (\text{B.7})$$

C Shadow Property

C.1 Proof of Theorem 5

Proof. First, consider the vector field of the symplectified system (2.7),

$$\begin{aligned} X_H &= \frac{\partial \mathcal{H}}{\partial P_I} \frac{\partial}{\partial Q^I} - \frac{\partial \mathcal{H}}{\partial Q^I} \frac{\partial}{\partial P_I} \\ &= \frac{\partial}{\partial q^0} - \frac{\partial H_{\text{total}}}{\partial q^0} \frac{\partial}{\partial p_0} + X_H - \psi_a \frac{\partial}{\partial \pi_a} \\ &\approx \frac{\partial}{\partial q^0} - \frac{\partial H}{\partial q^0} \frac{\partial}{\partial p_0} + X_H, \end{aligned} \quad (\text{C.1})$$

where the last equality holds on the constraint surface $\psi_a(t, \mathbf{q}, \mathbf{p}) = 0$ ($a = 1, \dots, m$). The flow of the first two terms yield

$$\frac{dq^0}{ds} = 1, \quad \frac{dp_0}{ds} = -\frac{\partial H}{\partial q^0} = -\frac{dH}{ds}, \quad (\text{C.2})$$

where we have made use of (2.3). Thus,

$$q^0(s) = s, \quad p_0(s) = -H(s) + H(0) + p_0(0) \approx -H(s) + \mathcal{H}(0), \quad (\text{C.3})$$

provided $q^0(0) = 0$, which fixes $q^0 = t = s$. The Hamiltonian is determined up to an arbitrary constant, and it is convenient to take $\mathcal{H}(0) = 0$ since then p_0 simply corresponds to the value $-H(s)$ at a given instant of time. Thus, we have precisely the ‘‘gauge fixing’’ of Eq. (2.8).

A presymplectic integrator (see Definition 3) is a *restricted symplectic integrator* Φ_h applied to the higher-dimensional system (2.7). Let $\widehat{\varphi}_s$ denote the true flow of $X_{\mathcal{H}}$. Because Φ_h is symplectic, and moreover it is a variational integrator (see Assumption 4), it holds globally that [19, 26]

$$\mathcal{H} \circ \Phi_h^\ell = \mathcal{H} \circ \widehat{\varphi}_{h\ell} + \mathcal{O}(h^r) \quad (\text{C.4})$$

for $s_\ell = \ell h = \mathcal{O}(h^r e^{c/h})$, $\ell = 0, 1, \dots$, and some constant $c > 0$. Recall that q^0 is just the time parameter, which is integrated exactly, and p_0 is a function of time alone and it does not couple to the other degrees of freedom, thus it is also integrated exactly (this was noted in [37, 38] as well). Denote

$$\mathbf{Z} \equiv (q^0, p_0, q^i, p_i), \quad \mathbf{z} \equiv (q^i, p_i), \quad \mathbf{Z}_\bullet \equiv \mathbf{Z}(s=0). \quad (\text{C.5})$$

We have

$$q_\ell^0 \equiv (q^0 \circ \Phi_h^\ell)(\mathbf{Z}_\bullet) = q^0 \circ \widehat{\varphi}_{h\ell}(\mathbf{Z}_\bullet) = h\ell, \quad (\text{C.6})$$

i.e., we just used the fact that Φ_h integrates q^0 exactly. Similarly,

$$p_{0,\ell} \equiv (p_0 \circ \Phi_h^\ell)(\mathbf{Z}_\bullet) = p_0 \circ \widehat{\varphi}_{h\ell}(\mathbf{Z}_\bullet) = p_0(h\ell), \quad (\text{C.7})$$

which is however irrelevant since this term does not couple to the other degrees of freedom. On the constraint surface $\mathcal{H} \approx H(q^0, q^i, p_i)$, which is a function on $\mathbb{R} \times T^*\mathcal{Q}$, the extended cotangent bundle of the base manifold \mathcal{Q} . Define the projection

$$\begin{aligned} \pi : \mathbb{R}^2 \times T^*\mathcal{Q} &\rightarrow \mathbb{R} \times T^*\mathcal{Q} \\ \mathbf{Z} &\mapsto (q^0, \mathbf{z}), \end{aligned} \quad (\text{C.8})$$

which eliminates p_0 . We can write

$$\mathcal{H} \approx p_0 + H \circ \pi \quad (\text{C.9})$$

and

$$\pi \circ \widehat{\varphi}_{hl} = \varphi_{hl} \circ \pi, \quad (\text{C.10a})$$

$$\pi \circ \Phi_h^\ell = \phi_h^\ell \circ \pi, \quad (\text{C.10b})$$

where φ_t denotes the true flow of the original dissipative Hamiltonian system on $\mathbb{R} \times T^*\mathcal{Q}$, and ϕ_h^ℓ denotes ℓ iterations of the *presymplectic* integrator ϕ_h on $\mathbb{R} \times T^*\mathcal{Q}$. Hence, from (C.4) and (C.9),

$$p_0 \circ \Phi_h^\ell + H \circ \pi \circ \Phi_h^\ell = p_0 \circ \widehat{\varphi}_{hl} + H \circ \varphi_{hl} \circ \pi + \mathcal{O}(h^r), \quad (\text{C.11})$$

where we used (C.10a) on the 2nd term of the RHS. Due to (C.7) we obtain

$$H \circ \pi \circ \Phi_h^\ell = H \circ \varphi_{hl} \circ \pi + \mathcal{O}(h^r), \quad (\text{C.12})$$

and upon using (C.10b) on the LHS we finally have

$$H \circ \phi_h^\ell = H \circ \varphi_{hl} + \mathcal{O}(h^r). \quad (\text{C.13})$$

This proves the relation (2.12), which is thus a consequence of (C.4) (shadow) and the symplectification. It should be noted, however, that this derivation assumes that all numerical maps and the Hamiltonian are globally defined, which is implicit under Assumption 4.

The above argument shows that the value of the nonconserved Hamiltonian H along the presymplectic integrator stays close to its true value. Furthermore, from the shadow expansion

$$\widetilde{\mathcal{H}} = \mathcal{H} + h^r \Delta \mathcal{H}_r + \dots, \quad (\text{C.14})$$

assumed to exist for the symplectic integrator Φ_h applied to the conserved Hamiltonian \mathcal{H} since it is a variational integrator, upon using (C.9) and (C.7) we conclude that there exists a *shadow nonconservative Hamiltonian* \widetilde{H} given by

$$\widetilde{H} = H + h^r \Delta H_r + \dots. \quad (\text{C.15})$$

■

The next result is a consequence of this shadow property and shows that presymplectic discretizations of system (3.2) are able to closely reproduce its convergence rates, whatever they are.

C.2 Proof of Corollary 6

Proof. Suppose the generic Hamiltonian system (3.2) has a rate of convergence of the form

$$f(\mathbf{q}(t)) - f(\mathbf{q}_\star) = \mathcal{O}(R(t)) \quad (\text{C.16})$$

for some decreasing function $R(t) > 0$, which tells us how fast the system converges to a minimum of the objective functions f . One would like to preserve such a convergence rate under discretization. Let ϕ_h be a presymplectic integrator of order $r \geq 1$ (Definition 3). It then holds that [39]

$$\|\phi_h^\ell(\mathbf{z}_\bullet) - \varphi_{t_\ell}(\mathbf{z}_\bullet)\| \leq C_\ell h^r \quad (\text{C.17})$$

for some constant $C_\ell > 0$ and sufficiently small step size $h > 0$, where $\mathbf{z}_\bullet \equiv (q^i(0), p_i(0))$ is the initial state, $t_\ell = h\ell$ is the simulation time ($\ell = 0, 1, \dots$), and we recall that φ_t is the true

flow. Note also that $\|\cdot\|$ in (C.17) represents some norm defined over the manifold $T^*\mathcal{Q}$ [39]. Replacing the Hamiltonian (3.1), i.e., $H = \frac{1}{2}e^{-\eta(t)}g^{ij}p_i p_j + e^{\eta(t)}f(q)$, into Eq. (2.12) yields

$$f \circ \phi_h^\ell - f \circ \varphi_{h\ell} = e^{-2\eta(t_\ell)}(T \circ \varphi_{h\ell} - T \circ \phi_h^\ell) + e^{-\eta(t_\ell)}h^r K, \quad (\text{C.18})$$

for some constant $K > 0$ and where $T \equiv \frac{1}{2}\mathbf{p} \cdot \mathbf{g}^{-1}(\mathbf{q})\mathbf{p}$ is the kinetic energy. Due to the smoothness of the Riemannian manifold \mathcal{Q} and (C.17) we have the Lipschitz condition

$$|(T \circ \varphi_{h\ell} - T \circ \phi_h^\ell)| \leq L_T C_\ell h^r, \quad (\text{C.19})$$

for some constant $L_T > 0$. Therefore,

$$|f \circ \phi_h^\ell - f \circ \varphi_{h\ell}| \leq e^{-\eta(t_\ell)}h^r (L_T C_\ell e^{-\eta(t_\ell)} + K). \quad (\text{C.20})$$

The result (3.3) follows provided $C_\ell e^{-\eta(t_\ell)}$ is finite. Let us use a pretty conservative bound on C_ℓ , for instance on \mathbb{R}^n it is common to have $C_\ell = C(e^{L_\phi t_\ell} - 1)$, where L_ϕ is a Lipschitz constant of the integrator [23], i.e., $\|\phi_h(z_1) - \phi_h(z_2)\| \leq L_\phi \|z_1 - z_2\|$, and $C > 0$ is a constant that does not depend on ℓ . Such a bound holds for the majority of methods, even nonstructure-preserving ones. Thus, under such a growth condition on C_ℓ and by the assumption in the theorem, i.e., $e^{L_\phi t_\ell - \eta(t_\ell)} < \infty$, we conclude that

$$\underbrace{R_\ell}_{\text{discrete}} = \underbrace{R(h\ell)}_{\text{continuum}} + \underbrace{\mathcal{O}(e^{-\eta(t_\ell)}h^r)}_{\text{small error}} \quad (\text{C.21})$$

during suitable simulation times as stated in Theorem 5. ■

D KKT Conditions and Stability

In this section, we describe the results related to the stability system (3.2), stated in Sec. 3. Such results extends immediately to system (4.6) which incorporates inequality constraints. We start by characterizing critical points in terms of the KKT conditions.

D.1 Proof of Theorem 7

Proof. The system (3.2) can be written in first order form as

$$\dot{q}^i = g^{ij}(\mathbf{q})p_j, \quad (\text{D.1a})$$

$$\dot{p}_i = -\dot{\eta}(t)p_i - \frac{1}{2}\partial_i g^{jk}(\mathbf{q})p_j p_k - \partial_i f(\mathbf{q}) - \lambda^a \partial_i \psi_a(\mathbf{q}), \quad (\text{D.1b})$$

$$0 = \psi_a(\mathbf{q}). \quad (\text{D.1c})$$

By definition, a critical point $(\mathbf{q}_*, \boldsymbol{\lambda}_*, \mathbf{p}^*)$ is such that the vector field on the RHS vanishes, namely $p_i^* = 0$, $\psi_a(\mathbf{q}_*) = 0$, and $\partial_i f(\mathbf{q}_*) + \lambda_*^a \partial_i \psi_a(\mathbf{q}_*) = 0$, for all $i = 1, \dots, n$ and $a = 1, \dots, m$. The last two relations are precisely the KKT conditions for the optimization problem (3.4). ■

This result shows that critical points of system (D.1) obey the KKT conditions, which are the first order *necessary* conditions for optimality. Recall that if the system converges, it must do so to a critical point.

D.2 Extension to inequality constraints

Let us also show that the previous result extends to system (4.6) with more general KKT conditions.

Theorem 10. *Let $(\mathbf{q}_\star, \boldsymbol{\lambda}_\star, \boldsymbol{\mu}_\star)$ (and $\mathbf{p}^\star = \mathbf{0}$) be a critical point of system (4.6). Then such a critical point must obey the KKT conditions for the optimization problem*

$$\min_{\mathbf{q} \in \mathcal{M}} f(\mathbf{q}) \quad \text{s.t.} \quad \boldsymbol{\psi}(\mathbf{q}) = \mathbf{0}, \quad \boldsymbol{\phi}(\mathbf{q}) \leq \mathbf{0}, \quad (\text{D.2})$$

namely

$$\partial_i f(\mathbf{q}_\star) + \lambda_\star^a \partial_i \psi_a(\mathbf{q}_\star) + \mu_\star^b \partial_i \phi_b(\mathbf{q}_\star) = 0 \quad (\text{stationarity}), \quad (\text{D.3a})$$

$$\psi_a(\mathbf{q}_\star) = 0, \quad \phi_b(\mathbf{q}_\star) \leq 0 \quad (\text{primal feasibility}), \quad (\text{D.3b})$$

$$\mu_\star^b \cdot \phi_b(\mathbf{q}_\star) = 0 \quad (\text{complementary slackness}), \quad (\text{D.3c})$$

$$\mu_\star^b \geq 0 \quad (\text{dual feasibility}), \quad (\text{D.3d})$$

where $i = 1, \dots, n$, $a = 1, \dots, m$, and $b = 1, \dots, \bar{m}$.

Proof. We can write system (4.6) in first order as

$$\dot{q}^i = g^{ij}(\mathbf{q}) p_j, \quad (\text{D.4a})$$

$$\dot{p}_i = -\dot{\eta}(t) p_i - \frac{1}{2} \partial_i g^{jk}(\mathbf{q}) p_j p_k - \partial_i f(\mathbf{q}) - \lambda^a \partial_i \psi_a(\mathbf{q}) - \mu^b \partial_i \phi_b(\mathbf{q}), \quad (\text{D.4b})$$

$$0 = \psi_a(\mathbf{q}), \quad (\text{D.4c})$$

$$0 = \phi_b(\mathbf{q}), \quad (\text{D.4d})$$

under the condition that $\mu^b(t) = 0$ when $\phi_b(\mathbf{q}(t)) < 0$, i.e., when an inequality constraint is *inactive* it does not participate in the dynamics and the system becomes unconstrained with respect to ϕ_b .

A critical point is a zero of the RHS of (D.4), thus it must obey $p_i^\star = 0$, $\psi_a(\mathbf{q}_\star) = 0$, $\phi_b(\mathbf{q}_\star) = 0$, and $\partial_i f(\mathbf{q}_\star) + \lambda_\star^a \partial_i \psi_a(\mathbf{q}_\star) + \mu_\star^b \partial_i \phi_b(\mathbf{q}_\star) = 0$. Note also that when $\mu_\star^b = 0$ we have $\phi_b(\mathbf{q}_\star) < 0$, so the inequality $\phi_b(\mathbf{q}_\star) \leq 0$ is obeyed. Hence, the KKT conditions (D.3a) and (D.3b) are satisfied. Moreover, the dynamics is defined in such a way that $\mu^b(t) \cdot \phi_b(\mathbf{q}(t)) = 0$ at all times, and this holds in particular at the critical point, thus condition (D.3c) is obeyed. Finally, as a consequence of this last equality, it was already shown in (4.3) and (4.4) that condition (D.3d) follows. \blacksquare

D.3 Proof of Theorem 8

We now consider Lyapunov stability. Note that it is implicit that $\dot{\eta}(t) > 0$ in order to have a dissipative system—if $\dot{\eta}(t) < 0$ the system would be excited, i.e., energy would be pumped into the system, and if $\dot{\eta}(t) = 0$ the system would be conservative.

Proof. Consider system (3.2) written in first order form, i.e., Eq. (D.1) which we write as

$$\dot{q}^i \approx g^{ij} p_j, \quad \dot{p}_i \approx -\dot{\eta}(t) p_i - \frac{1}{2} \partial_i g^{jk} p_j p_k - \partial_i f - \lambda^a \partial_i \psi_a \quad (\text{D.5})$$

following Dirac's notation. Without loss of generality, assume the critical point of interest is at the origin, $\mathbf{q}_\star = \mathbf{0}$, and that the minimum is achieved with value $f(\mathbf{q}_\star) = \min_{\mathbf{q} \in \mathcal{M}} f(\mathbf{q}) = 0$.

Furthermore, assume that the critical point is *isolated*, namely there exists a neighborhood of $(\mathbf{p}^* = \mathbf{0}, \mathbf{q}_* = \mathbf{0}, \boldsymbol{\lambda}_*)$ such that the system has no other critical point except for this one. Now consider the function

$$\mathcal{E}(\mathbf{q}, \mathbf{p}, \boldsymbol{\lambda}) \equiv \frac{1}{2}g^{ij}(\mathbf{q})p_i p_j + f(\mathbf{q}) + \lambda^a \psi_a(\mathbf{q}). \quad (\text{D.6})$$

On the constraint surface, the last term is effectively zero, i.e., $\mathcal{E}(\mathbf{q}_*, \mathbf{p}^*, \boldsymbol{\lambda}_*) \approx 0$, and also

$$\mathcal{E}(\mathbf{q}, \mathbf{p}, \boldsymbol{\lambda}) > 0 \quad (\text{D.7})$$

for all points different than the critical point of interest. Thus \mathcal{E} is positive definite in a sufficiently small region around the critical point. Moreover, differentiating this function with respect to time and subbing the equations of motion, we conclude that

$$\dot{\mathcal{E}} = -\dot{\eta}(t)g^{ij}p_i p_j \leq 0. \quad (\text{D.8})$$

The function \mathcal{E} is therefore a Lyapunov function [40], which implies that the system is *stable* on such a critical point. In addition, if $\eta(t) = \gamma t$ for $\gamma = \text{constant} > 0$, then LaSalle's invariance principle [40] ensures that the system is *asymptotically stable* around the critical point, i.e., trajectories actually converge to the critical point. ■

The exact same argument applies to system (4.6) on the more general setting of problem (4.1), which accounts for inequality constraints. This is done by considering the Lyapunov function

$$\mathcal{E}(\mathbf{q}, \mathbf{p}, \boldsymbol{\lambda}, \boldsymbol{\mu}) \equiv \frac{1}{2}g^{ij}(\mathbf{q})p_i p_j + f(\mathbf{q}) + \lambda^a \psi_a(\mathbf{q}) + \mu^b \phi_b(\mathbf{q}). \quad (\text{D.9})$$

and making use of the equations of motion (D.4). The argument is unchanged since the inequality constraint $\phi_b(\mathbf{q})$ works effectively as an equality constraint, otherwise $\mu^b = 0$ and ϕ_b does not participate in the dynamics. Therefore, such a stability result remains valid in the presence of inequality constraints as well.

E Implicit Dynamics on the Constraint Surface and Convergence Rate

This section is perhaps the most technical, where we show the decay rates of systems (3.2) and (4.6) to localized minima in the feasible region of the constraints. The strategy is to solve explicitly for the Lagrange multipliers to obtain a differential equation that describes the implicit dynamics on the constraint surface.

We first consider the system (3.2) and explicitly solve for the Lagrange multipliers, thus reducing it into a differential equation that characterizes the dynamics on the constraint submanifold $\mathcal{Q} \subset \mathcal{M}$. Denoting $\gamma(t) = \dot{\eta}(t)$, the constrained dissipative geodesic equation of interest is

$$\ddot{q}^i + \Gamma^i_{jk} \dot{q}^j \dot{q}^k + \gamma(t) \dot{q}^i = -\partial^i f - \lambda_a \partial^i \psi^a, \quad \psi^a(\mathbf{q}) = 0. \quad (\text{E.1})$$

We are now denoting ψ^a with upper indices since we view this as a coordinate transformation. Define the ‘‘vielbein’’ fields [35, 36]

$$e^a{}_i \equiv \frac{\partial \psi^a}{\partial q^i}, \quad e_a{}^i \equiv \frac{\partial q^i}{\partial \psi^a}. \quad (\text{E.2})$$

They obey $e^a_i e_a^j = \delta_j^i$ and $e_a^i e^b_i = \delta_a^b$. The vielbein defines a metric on the constraint surface (together with its inverse) given by

$$G_{ab} \equiv e_a^i g_{ij} e_b^j, \quad G^{ab} \equiv e_a^i g^{ij} e_b^j. \quad (\text{E.3})$$

These objects appear in the ‘‘tetrad’’ formalism of general relativity [35].³ The constraint $\psi^a(\mathbf{q}) = 0$ gives rise to the so-called ‘‘hidden constraints’’ $d\psi^a/dt = 0$ and $d^2\psi^a/dt^2 = 0$ that yield

$$e^a_i \dot{q}^i = 0 \quad (\text{E.4})$$

and

$$e^a_i \ddot{q}^i + \partial_i e^a_j \dot{q}^i \dot{q}^j = 0. \quad (\text{E.5})$$

Replacing the first of Eq. (E.1) above allows us to solve for the Lagrange multipliers,

$$\lambda_c = G_{ca} \partial_i e^a_j \dot{q}^i \dot{q}^j - G_{ca} e^a_i \left(\Gamma^i_{jk} \dot{q}^j \dot{q}^k + \gamma \dot{q}^i + \partial^i f \right). \quad (\text{E.6})$$

Define the *projection* operators

$$\mathcal{P}_{\parallel}{}^{ij} \equiv g^{ij} - \mathcal{P}_{\perp}{}^{ij}, \quad \mathcal{P}_{\perp}{}^{ij} \equiv e_a^i G^{ab} e_b^j. \quad (\text{E.7})$$

One can check that they obey $\mathcal{P}_{\parallel}^2 = \mathcal{P}_{\parallel}$, $\mathcal{P}_{\perp}^2 = \mathcal{P}_{\perp}$, and $\mathcal{P}_{\parallel} \mathcal{P}_{\perp} = \mathcal{P}_{\perp} \mathcal{P}_{\parallel} = 0$. The vielbeins define the affine connection

$$\Gamma_{\perp}{}^i{}_{jk} \equiv e_a^i \partial_j e^a_k. \quad (\text{E.8})$$

Let us also define the projected connection

$$\Gamma_{\parallel}{}^i{}_{jk} \equiv \mathcal{P}_{\parallel}{}^i{}_{\ell} \Gamma^{\ell}{}_{jk}. \quad (\text{E.9})$$

One can also check that

$$\mathcal{P}_{\perp} \Gamma_{\perp} = \Gamma_{\perp}, \quad \mathcal{P}_{\parallel} \Gamma_{\perp} = 0, \quad \mathcal{P}_{\perp} \Gamma_{\parallel} = 0, \quad \mathcal{P}_{\parallel} \Gamma_{\parallel} = \Gamma_{\parallel}, \quad (\text{E.10})$$

and

$$\Gamma_{\perp} \mathcal{P}_{\perp} = \Gamma_{\perp}, \quad \Gamma_{\perp} \mathcal{P}_{\parallel} = 0, \quad \Gamma_{\parallel} \mathcal{P}_{\perp} = 0, \quad \Gamma_{\parallel} \mathcal{P}_{\parallel} = \Gamma_{\parallel}. \quad (\text{E.11})$$

Thus, Γ_{\parallel} is a connection on the constraint surface that defines the configuration manifold \mathcal{Q} , while Γ_{\perp} is a connection on its orthogonal complementary space. With these ingredients, we now obtain the following interesting result.

Theorem 11. *The differential algebraic equation (E.1) can be reduced to the differential equation*

$$\ddot{q}^i + \left(\Gamma_{\parallel}{}^i{}_{jk} + \Gamma_{\perp}{}^i{}_{jk} \right) \dot{q}^j \dot{q}^k + \gamma(t) \mathcal{P}_{\parallel}{}^i{}_j \dot{q}^j = -\mathcal{P}_{\parallel}{}^{ij} \partial_j f, \quad (\text{E.12})$$

which describes the implicit dynamics on the constraint subspace \mathcal{Q} (the configuration manifold) that is embedded into \mathcal{M} . Furthermore, the dynamics is orthogonally decoupled into a driven dissipative geodesic equation and a free geodesic equation, respectively given by

$$\mathcal{P}_{\parallel}{}^i{}_j \ddot{q}^j + \Gamma_{\parallel}{}^i{}_{jk} \dot{q}^j \dot{q}^k + \gamma(t) \mathcal{P}_{\parallel}{}^i{}_j \dot{q}^j = -\mathcal{P}_{\parallel}{}^{ij} \partial_j f, \quad (\text{E.13a})$$

$$\mathcal{P}_{\perp}{}^i{}_j \ddot{q}^j + \Gamma_{\perp}{}^i{}_{jk} \dot{q}^j \dot{q}^k = 0. \quad (\text{E.13b})$$

³In the same way that g_{ij} lowers indices of the q^j coordinates, G_{ab} lowers indices of the ψ^b coordinates—and similarly g^{ij} and G^{ab} raises indices of coordinates q_j and ψ_b , respectively. The expressions (E.3) can be seen as a change of metric, $g \mapsto G$, in going from \mathcal{M} to \mathcal{Q} .

Proof. Eq. (E.12) follows by replacing the explicit form of the Lagrange multipliers (E.6) into (E.1) and using definitions (E.7)–(E.9). Eqs. (E.13) follow from Eq. (E.12) by acting with \mathcal{P}_\parallel and \mathcal{P}_\perp upon using the properties of these projection operators and relations (E.10). ■

This result is completely general and may be of independent interest, e.g., it can provide the starting point to study the dynamics on more general manifold and constrained optimization problems (3.4) and (4.1). Note that (E.12) and (E.13) no longer have mention to Lagrange multipliers; these equations have instead projection operators to the constraint surface and its orthogonal complement. Moreover, Eq. (E.13b) is a free geodesic motion. It implies that if the system is initialized on the constraint surface then it remains on this surface at all times, i.e., if $\mathbf{q}(0) = \mathcal{P}_\parallel \mathbf{q}(0)$ and $\dot{\mathbf{q}}(0) = \mathcal{P}_\parallel \dot{\mathbf{q}}(0)$ then $\mathcal{P}_\perp \mathbf{q}(t) = 0$ and $\mathcal{P}_\perp \dot{\mathbf{q}}(t) = 0$. In this case, the dynamics is completely determined by Eq. (E.13a) alone. Based on this decomposition, we can finally study convergence to equilibrium using stability theory since we have reduced the problem to the analysis of a *differential equation*.

E.1 Proof of Theorem 9

Proof. By assumption, the initial state $\mathbf{q}(0) \equiv \mathbf{q}_0$ and $\dot{\mathbf{q}}(0) = \mathbf{0}$ is on the constraint surface, therefore the dynamics is completely specified by Eq. (E.13a). We have

$$\mathbf{q} = \mathcal{P}_\parallel \mathbf{q}, \quad \dot{\mathbf{q}} \equiv \mathcal{P}_\parallel \dot{\mathbf{q}}, \quad \ddot{\mathbf{q}} \equiv \mathcal{P}_\parallel \ddot{\mathbf{q}}, \quad (\text{E.14})$$

since the state never leaves the constraint submanifold. Making use of the last equation in (E.11) we can write

$$\ddot{q}^i + \Gamma_{\parallel}^i{}_{jk}(\mathbf{q}) \dot{q}^j \dot{q}^k + \gamma \dot{q}^i = -\mathcal{P}_\parallel(\mathbf{q})^{ij} \partial_j f(\mathbf{q}), \quad (\text{E.15})$$

where here we consider $\gamma > 0$ constant. We are interested in studying the system around an isolated critical point $\mathbf{q}_\star = \mathbf{0}$, assumed to be at the origin without loss of generality, and which by definition obeys

$$\mathcal{P}_\parallel(\mathbf{q}_\star)^{ij} \partial_j f(\mathbf{q}_\star) = 0. \quad (\text{E.16})$$

A key result from stability theory is the Hartman-Grobman theorem [41], allowing us to linearize the system around \mathbf{q}_\star (the equilibrium is nondegenerate/hyperbolic by assumption). Moreover, in a neighborhood of this point, there always exists Riemann normal coordinates such that the connection vanishes, $\Gamma^i{}_{jk} = 0$ [35, 36]. This is the mathematical statement of the “equivalent principle” from general relativity. Additionally, the metric g_{ij} can be taken to be the identity, δ_{ij} , although for our purposes we allow it to be a constant metric. Using (E.14) we thus have

$$\ddot{q}^i + \gamma \dot{q}^i = -\mathcal{P}_\parallel(\mathbf{q})^{ij} \partial_j f(\mathcal{P}_\parallel \mathbf{q}). \quad (\text{E.17})$$

Expanding the RHS of this equation around \mathbf{q}_\star we have the linearized system

$$\ddot{q}^i + \gamma \dot{q}^i = -\mathcal{P}_\parallel(\mathbf{q}_\star)^{ij} \partial_j \partial_k f(\mathbf{q}_\star) \mathcal{P}_\parallel(\mathbf{q}_\star)^k{}_\ell q^\ell, \quad (\text{E.18})$$

Note that \mathcal{P}_\parallel defined in (E.7) is symmetric, therefore the operator on the RHS of (E.18) is (real) symmetric and can be diagonalized by an orthogonal transformation. Denote

$$H_\parallel \equiv (\mathcal{P}_\parallel \nabla^2 f \mathcal{P}_\parallel)|_{\mathbf{q}_\star} \quad (\text{E.19})$$

the *projected Hessian* at the critical point. Letting $H_\parallel = O^T \Omega O$ be its diagonalization, and defining $\mathbf{x} = O \mathbf{q}$, the components of the differential equation (E.18) can decoupled and we are left with several one-dimension problems of the form

$$\ddot{x} + \gamma \dot{x} = -\omega x, \quad \omega \equiv \lambda(H_\parallel), \quad (\text{E.20})$$

where ω denotes an eigenvalue of (E.19). Around an isolated minimizer, all these eigenvalues are positive. Hence, the *slowest* degree of freedom of the system obeys this differential equation with ω_{\min} , the smallest eigenvalue, which has solution

$$x(t) = C_+ e^{\xi+t} + C_- e^{\xi-t}, \quad \xi = \frac{-\gamma \pm \sqrt{\gamma^2 - 4\omega_{\min}}}{2}, \quad (\text{E.21})$$

for constants C_{\pm} depending on the initial conditions \mathbf{q}_0 and $\dot{\mathbf{q}}(0) = \mathbf{0}$. Choosing $\gamma \leq 2\sqrt{\omega_{\min}}$ (underdamped and critically damped regimes), from this exact solution we conclude that for all components of the system we have

$$\|\mathbf{q}(t) - \mathbf{q}_*\| \leq \|\mathbf{q}_0 - \mathbf{q}_*\| e^{-\sqrt{\omega_{\min}}t}. \quad (\text{E.22})$$

This shows the result (3.6) in terms of the smallest eigenvalue of the projected Hessian (E.19).

To make connection with the operator (5.3), consider explicitly the matrix representation of \mathcal{P}_{\parallel} in general. From the definition (E.7) we have

$$\begin{aligned} \mathcal{P}_{\parallel}^{ij} &= g^{ij} - g^{ik} e^a_k G_{ab} e^b_{\ell} g^{\ell j} \\ &= g^{ik} \left(\delta_k^j - e^a_k G_{ab} e^b_{\ell} g^{\ell j} \right). \end{aligned} \quad (\text{E.23})$$

In our notation, $\mathcal{J}_i^a = \partial\psi^a/\partial q^i = e^a_i$ is the $m \times n$ Jacobian matrix of constraints, g^{ij} is the $n \times n$ inverse metric $(g^{-1})_{ij}$, and G_{ab} the $m \times m$ inverse matrix of $(G^{-1})^{ab}$. From (E.3) we have

$$G^{-1} = \mathcal{J}g^{-1}\mathcal{J}^T \equiv \mathcal{R}. \quad (\text{E.24})$$

We can thus write (E.23) in matrix form as

$$\mathcal{P}_{\parallel} = g^{-1} (I - \mathcal{J}^T \mathcal{R}^{-1} \mathcal{J} g^{-1}) = g^{-1} \mathcal{P} \quad (\text{E.25})$$

in terms of the operator \mathcal{P} defined in (5.3). Thus, the above eigenvalue can be alternatively represented by

$$\omega_{\min} \equiv \lambda_{\min} \left((g^{-1} \mathcal{P} \nabla^2 f \mathcal{P}^T g^{-1})|_{\mathbf{q}_*} \right). \quad (\text{E.26})$$

If we had fixed the metric to be Euclidean, $g_{ij}|_{\mathbf{q}_*} = \delta_{ij}$, then $\mathcal{P}_{\parallel} = \mathcal{P}$ at \mathbf{q}_* . ■

Interestingly, the above result provides a local accelerated convergence rate and it does not require the Hessian of f to be positive definite, i.e., it requires that the *projected Hessian* in (E.26) is positive definite, which allows f and the constraints to be *nonconvex*.

In light of the previous discussions related to system (4.6) that accounts for the inequality constraints of problem (4.1) (see, e.g., Eq. (D.4)), we know that inequality constraints are only active when they are actually equality constraints. Therefore, the above result extends immediately to this case as well, with the full operator (5.3) incorporating the nonlinear constraints.

F Derivation of Dissipative RATTLE for Constrained Optimization

Here we derive the algorithm introduced in Sec. 5. We first consider the standard RATTLE integrator applied to conservative systems. Then we reduce this method to our dissipative and constrained case. We will then introduce a modification of this method that is more efficient.

F.1 Dissipative RATTLE

Following Definition 3, we first consider a symplectic integrator to conservative and constrained systems based on the standard RATTLE method [28]; this method is known to be symplectic [29, 30] and it is also a variational integrator (see Assumption 4). This method has order of accuracy $r = 2$. Thus, consider a generic conservative and constrained system with total Hamiltonian $\mathcal{H}_{\text{total}} = \mathcal{H}(q^\mu, p_\mu) + \lambda^a \psi_a(q^\mu)$, where $\mu = 0, 1, \dots, n$ and the constraints are holonomic. We use the general form of this method written in [23] that reads

$$p_{\mu, \ell+1/2} = p_{\mu, \ell} - \frac{h}{2} \left[\frac{\partial \mathcal{H}}{\partial q^\mu}(\mathbf{q}_\ell, \mathbf{p}_{\ell+1/2}) + \lambda_\ell^a \frac{\partial \psi_a}{\partial q^\mu}(\mathbf{q}_\ell) \right], \quad (\text{F.1a})$$

$$q_{\ell+1}^\mu = q_\ell^\mu + \frac{h}{2} \left[\frac{\partial \mathcal{H}}{\partial p_\mu}(\mathbf{q}_\ell, \mathbf{p}_{\ell+1/2}) + \frac{\partial \mathcal{H}}{\partial p_\mu}(\mathbf{q}_{\ell+1}, \mathbf{p}_{\ell+1/2}) \right], \quad (\text{F.1b})$$

$$0 = \psi_a(\mathbf{q}_{\ell+1}) \quad (a = 1, \dots, m), \quad (\text{F.1c})$$

$$p_{\mu, \ell+1} = p_{\mu, \ell+1/2} - \frac{h}{2} \left[\frac{\partial \mathcal{H}}{\partial q^\mu}(\mathbf{q}_{\ell+1}, \mathbf{p}_{\ell+1/2}) + \rho_\ell^a \frac{\partial \psi_a}{\partial q^\mu}(\mathbf{q}_{\ell+1}) \right], \quad (\text{F.1d})$$

$$0 = \frac{\partial \psi_a}{\partial q^\mu}(\mathbf{q}_{\ell+1}) \frac{\partial \mathcal{H}}{\partial p_\mu}(\mathbf{q}_{\ell+1}, \mathbf{p}_{\ell+1}) \quad (a = 1, \dots, m), \quad (\text{F.1e})$$

where $\ell = 0, 1, \dots$ is the iteration number. Note that we introduced additional Lagrange multipliers ρ^a associated to the so-called ‘‘hidden constraints’’

$$0 = \frac{d\psi_a}{ds} = \frac{\partial \psi_a}{\partial q^\mu} \frac{dq^\mu}{ds} = \frac{\partial \psi_a}{\partial q^\mu} \frac{d\mathcal{H}}{dp_\mu}, \quad (\text{F.2})$$

which forces the velocity dq^μ/ds to be tangent to the constraint surface.⁴ This condition is not strictly necessary, but it results in a more stable integrator.

According to Definition 3, to obtain a method for system (3.1), all we have to do is set $q_\ell^0 = t_\ell = s_\ell = h\ell$ into (F.1) and forget about p_0 since it does not couple to the other degrees of freedom; recall the gauge fixing (2.8). Moreover, to avoid dealing with implicit schemes in this paper, we will assume that the metric $g_{ij}(\mathbf{q})$ is constant, i.e., independent of \mathbf{q} , so that all updates become explicit. We thus obtain

$$p_{i, \ell+1/2} = p_{i, \ell} - \frac{h}{2} e^{\eta(t_\ell)} \left[\frac{\partial f(\mathbf{q}_\ell)}{\partial q^i} + \lambda_\ell^a \frac{\partial \psi_a(\mathbf{q}_\ell)}{\partial q^i} \right], \quad (\text{F.3a})$$

$$t_{\ell+1} = t_\ell + h, \quad (\text{F.3b})$$

$$q_{\ell+1}^i = q_\ell^i + \frac{h}{2} \left[e^{-\eta(t_\ell)} + e^{-\eta(t_{\ell+1})} \right] g^{ij} p_{j, \ell+1/2}, \quad (\text{F.3c})$$

$$0 = \psi_a(\mathbf{q}_{\ell+1}) \quad (a = 1, \dots, m), \quad (\text{F.3d})$$

$$p_{i, \ell+1} = p_{i, \ell+1/2} - \frac{h}{2} e^{\eta(t_{\ell+1})} \left[\frac{\partial f(\mathbf{q}_{\ell+1})}{\partial q^i} + \rho_\ell^a \frac{\partial \psi_a(\mathbf{q}_{\ell+1})}{\partial q^i} \right], \quad (\text{F.3e})$$

$$0 = \frac{\partial \psi_a(\mathbf{q}_{\ell+1})}{\partial q^i} g^{ij} p_{j, \ell+1} \quad (a = 1, \dots, m). \quad (\text{F.3f})$$

Redefining the momentum variable as

$$e^{-\eta(t_\ell)} \mathbf{p}_\ell \mapsto \mathbf{p}_\ell, \quad (\text{F.4})$$

⁴We note that we are implicitly assuming that the Lagrange multipliers can be uniquely determined, which is guaranteed when $\partial_{\mathbf{q}} \psi(\partial_{\mathbf{p}\mathbf{p}} \mathcal{H}) \partial_{\mathbf{q}} \psi^T$ is invertible. This condition is standard and also assumed for all constrained symplectic integrators in the literature.

and also defining the functions

$$\alpha_{\ell+1/2} \equiv e^{-(\eta(t_{\ell+1/2})-\eta(t_\ell))} \quad (\text{F.5})$$

and

$$\beta_{\ell+1} \equiv \frac{e^{\eta(t_{\ell+1/2})-\eta(t_\ell)} + e^{-(\eta(t_{\ell+1})-\eta(t_{\ell+1/2}))}}{2} = \frac{(\alpha_{\ell+1/2})^{-1} + \alpha_{\ell+1}}{2}, \quad (\text{F.6})$$

we can write (F.3) as

$$\mathbf{p}_{\ell+1/2} = \alpha_{\ell+1/2} [\mathbf{p}_\ell - (h/2)\nabla f(\mathbf{q}_\ell) - (h/2)\mathcal{J}(\mathbf{q}_\ell)^T \boldsymbol{\lambda}_\ell], \quad (\text{F.7a})$$

$$\mathbf{q}_{\ell+1} = \mathbf{q}_\ell + h\beta_{\ell+1}g^{-1}\mathbf{p}_{\ell+1/2}, \quad (\text{F.7b})$$

$$\mathbf{0} = \boldsymbol{\psi}(\mathbf{q}_{\ell+1}), \quad (\text{F.7c})$$

$$\mathbf{p}_{\ell+1} = \mathcal{P}(\mathbf{q}_{\ell+1}) [\alpha_{\ell+1}\mathbf{p}_{\ell+1/2} - (h/2)\nabla f(\mathbf{q}_{\ell+1})], \quad (\text{F.7d})$$

Note that we wrote the method in vectorial form, and some points need clarification. For instance, $\mathcal{J}(\mathbf{q})$ denotes the Jacobian matrix of constraints, $\mathcal{J}_{ai}(\mathbf{q}) \equiv \partial\psi_a/\partial q^i|_{\mathbf{q}}$, and we introduced the projection operator

$$\mathcal{P}(\mathbf{q}) \equiv I - \mathcal{J}(\mathbf{q})^T \mathcal{R}(\mathbf{q})^{-1} \mathcal{J}(\mathbf{q}) g^{-1}, \quad \mathcal{R}(\mathbf{q}) \equiv \mathcal{J}(\mathbf{q}) g^{-1} \mathcal{J}(\mathbf{q})^T. \quad (\text{F.8})$$

This operator arises when solving (F.3f) explicitly, i.e., replacing (F.3e) into (F.3f) and solving for the Lagrange multipliers $\boldsymbol{\rho}$. The Lagrange multipliers $\boldsymbol{\lambda}$ are obtained by solving (F.7c) numerically, i.e., the first three updates are solved simultaneously. Note also that we left the function $\eta(t)$ completely arbitrary.

The above method proved to be very efficient in our experiments. However, we use it as a stepping stone to construct an even more interesting method below, with the same computational cost.

F.2 Dissipative geodesic RATTLE

It is interesting to consider a more modern formulations of RATTLE as proposed in molecular dynamics [31]. When the Hamiltonian is separable, it is convenient to split the potential and kinetic contributions since the flow of the former can be integrated exactly, while the flow of the latter corresponds to a free geodesic motion on the constraint surface. Thus, consider the constrained Hamiltonian

$$\mathcal{H} = \frac{1}{2}e^{-\eta(q^0)}g^{ij}p_i p_j + e^{\eta(q^0)}f(q^i) + e^{\eta(q^0)}\lambda^a\psi_a(q^i) + p_0, \quad (\text{F.9})$$

which we will split with the sub-Hamiltonians

$$\mathcal{H} = \mathcal{H}_1 + \mathcal{H}_2, \quad (\text{F.10a})$$

$$\mathcal{H}_1 = e^{\eta(q^0)}f(q^i) + e^{\eta(q^0)}\nu^a\psi_a(q^i), \quad (\text{F.10b})$$

$$\mathcal{H}_2 = \frac{1}{2}e^{-\eta(q^0)}g^{ij}p_i p_j + e^{\eta(q^0)}\lambda^a\psi_a(q^i) + p_0, \quad (\text{F.10c})$$

where we introduced new multipliers ν^a in \mathcal{H}_1 —the value of the Lagrange multipliers are irrelevant when the constraints are satisfied. Consider the composition

$$e^{h\mathcal{L}_{\mathcal{H}}} = e^{(h/2)\mathcal{L}_{\mathcal{H}_1}} e^{h\mathcal{L}_{\mathcal{H}_2}} e^{(h/2)\mathcal{L}_{\mathcal{H}_1}} + \mathcal{O}(h^3), \quad (\text{F.11})$$

where $\mathcal{L}_{\mathcal{H}}$ denotes the Lie derivative along the flow of \mathcal{H} . As will be clear shortly, the flow of \mathcal{H}_1 can be integrated exactly, and we can replace any second order integrator to approximate the flow of \mathcal{H}_2 without spoiling the error in this approximation; we will use the dissipative version of RATTLE obtained in (F.3).

The equations of motion related to (F.10b) are

$$\frac{dq^i}{ds} = 0, \quad \frac{dq^0}{ds} = 0, \quad \frac{dp_i}{ds} = e^{\eta(q^0)} \left(\frac{\partial f}{\partial q^i} + \nu^a \frac{\partial \psi_a}{\partial q^i} \right), \quad \psi_a(\mathbf{q}) = 0. \quad (\text{F.12})$$

In these equations, only the momentum p_i evolves, thus the last equation is redundant if the initial position already satisfies the constraints. The original system (F.9) also satisfies the hidden constraints $d\psi_a/ds = 0$, i.e.,

$$\frac{\partial \psi_a}{\partial q^i} g^{ij} p_j = 0. \quad (\text{F.13})$$

Upon differentiating this equation with respect to time we can solve for the Lagrange multipliers ν^a explicitly, yielding

$$\frac{dp_i}{ds} = -e^{\eta(q^0)} \mathcal{P}_i^j \frac{\partial f}{\partial q^j}, \quad (\text{F.14})$$

where we have used the projection operator defined in Eq. (F.8). Since q^μ is constant we can integrate this equation exactly during a time interval Δs ,

$$p_i(s + \Delta s) = p_i(s) - (\Delta s) e^{\eta(q^0(s))} \mathcal{P}_i^j(\mathbf{q}(s)) \frac{\partial f(\mathbf{q}(s))}{\partial q^j}. \quad (\text{F.15})$$

The equations of motion related to (F.10c) are

$$\frac{dq^i}{ds} = e^{-\eta(q^0)} g^{ij} p_j, \quad \frac{dq^0}{ds} = 1, \quad \frac{dp_i}{ds} = -e^{\eta(q^0)} \lambda^a \frac{\partial \psi_a}{\partial q^i}, \quad \psi_a(\mathbf{q}) = 0. \quad (\text{F.16})$$

When we set $q^0 = s = t$ this corresponds to a free dissipative motion on the constraint surface, i.e., without an external potential. We can numerically solve these equations with the dissipative RATTLE proposed in (F.3) by setting $f = 0$. Thus, combining the exact solution (F.15) with the method (F.3) in approximating the composition (F.11), within the same $\mathcal{O}(h^3)$ local error, we obtain

$$\mathbf{p}_{\ell+1/2} = \mathbf{p}_\ell - (h/2) e^{\eta(t_\ell)} \mathcal{P}(\mathbf{q}_\ell) \nabla f(\mathbf{q}_\ell), \quad (\text{F.17a})$$

$$\tilde{\mathbf{p}}_{\ell+1/2} = \mathbf{p}_{\ell+1/2} - (h/2) e^{\eta(t_\ell)} \mathcal{J}(\mathbf{q}_\ell)^T \boldsymbol{\lambda}_\ell, \quad (\text{F.17b})$$

$$t_{\ell+1} = t_\ell + h, \quad (\text{F.17c})$$

$$\mathbf{q}_{\ell+1} = \mathbf{q}_\ell + (h/2) [e^{-\eta(t_\ell)} + e^{-\eta(t_{\ell+1})}] g^{-1} \tilde{\mathbf{p}}_{\ell+1/2}, \quad (\text{F.17d})$$

$$\mathbf{0} = \boldsymbol{\psi}(\mathbf{q}_{\ell+1}), \quad (\text{F.17e})$$

$$\tilde{\mathbf{p}}_{\ell+1} = \tilde{\mathbf{p}}_{\ell+1/2} - (h/2) \mathcal{J}(\mathbf{q}_{\ell+1})^T \boldsymbol{\rho}_\ell, \quad (\text{F.17f})$$

$$\mathbf{0} = \mathcal{J}(\mathbf{q}_{\ell+1}) g^{-1} \tilde{\mathbf{p}}_{\ell+1}, \quad (\text{F.17g})$$

$$\mathbf{p}_{\ell+1} = \tilde{\mathbf{p}}_{\ell+1} - (h/2) e^{-\eta(t_{\ell+1})} \mathcal{P}(\mathbf{q}_{\ell+1}) \nabla f(\mathbf{q}_{\ell+1}), \quad (\text{F.17h})$$

where \mathcal{J} is the Jacobian of constraints and we used the projection operator (F.8). We can further replace (F.17f) into (F.17g) and solve for $\boldsymbol{\rho}_\ell$ explicitly, resulting into $\tilde{\mathbf{p}}_{\ell+1} = \mathcal{P}(\mathbf{q}_{\ell+1}) \tilde{\mathbf{p}}_{\ell+1/2}$, which can now be directly combined with (F.17h) to obtain

$$\mathbf{p}_{\ell+1} = \mathcal{P}(\mathbf{q}_{\ell+1}) [\tilde{\mathbf{p}}_{\ell+1/2} - (h/2) e^{-\eta(t_{\ell+1})} \nabla f(\mathbf{q}_{\ell+1})]. \quad (\text{F.18})$$

Algorithm 2 DISSRATTLE is a presymplectic integrator for problem (5.1). The algorithm accepts a sequence of functions $\{\alpha_\ell\}$ where $\alpha_\ell \in (0, 1)$ (momentum factor) and step size $h > 0$. The parameter β_ℓ is fixed according to (F.6), and $g \succ 0$ is an arbitrary symmetric matrix (preconditioner).

```

1: for  $\ell = 0, 1, \dots$  do
2:    $\mathbf{p}_{\ell+1/2} \leftarrow \alpha_{\ell+1/2} \mathcal{P}(\mathbf{q}_\ell) [\mathbf{p}_\ell - (h/2) \nabla f(\mathbf{q}_\ell)]$ 
3:    $\tilde{\mathbf{p}}_{\ell+1/2} \leftarrow \mathbf{p}_{\ell+1/2} - (h\alpha_{\ell+1/2}/2) \mathcal{J}(\mathbf{q}_\ell)^T \Lambda_\ell$ 
4:    $\mathbf{q}_{\ell+1} \leftarrow \mathbf{q}_\ell + \beta_{\ell+1} g^{-1} \tilde{\mathbf{p}}_{\ell+1/2}$ 
5:   for  $a = 1, \dots, m + \tilde{m}$  do
6:     if  $\Psi_a$  is active then
7:        $\Lambda_{a,\ell} \leftarrow \Psi_a(\mathbf{q}_{\ell+1}) = 0$ 
8:     else
9:        $\Lambda_{a,\ell} \leftarrow 0$ 
10:    end if
11:  end for
12:   $\mathbf{p}_{\ell+1} \leftarrow \mathcal{P}(\mathbf{q}_{\ell+1}) [\alpha_{\ell+1} \tilde{\mathbf{p}}_{\ell+1/2} - (h/2) \nabla f(\mathbf{q}_{\ell+1})]$ 
13: end for

```

Using the functions (F.5) and (F.6), and introducing the change of momentum variable (F.4), we finally obtain

$$\mathbf{p}_{\ell+1/2} = \alpha_{\ell+1/2} \mathcal{P}(\mathbf{q}_\ell) [\mathbf{p}_\ell - (h/2) \nabla f(\mathbf{q}_\ell)], \quad (\text{F.19a})$$

$$\tilde{\mathbf{p}}_{\ell+1/2} = \mathbf{p}_{\ell+1/2} - (h\alpha_{\ell+1/2}/2) \mathcal{J}(\mathbf{q}_\ell)^T \boldsymbol{\lambda}_\ell, \quad (\text{F.19b})$$

$$\mathbf{q}_{\ell+1} = \mathbf{q}_\ell + h\beta_{\ell+1} g^{-1} \tilde{\mathbf{p}}_{\ell+1/2}, \quad (\text{F.19c})$$

$$\mathbf{0} = \boldsymbol{\psi}(\mathbf{q}_{\ell+1}), \quad (\text{F.19d})$$

$$\mathbf{p}_{\ell+1} = \mathcal{P}(\mathbf{q}_{\ell+1}) [\alpha_{\ell+1} \tilde{\mathbf{p}}_{\ell+1/2} - (h/2) \nabla f(\mathbf{q}_{\ell+1})]. \quad (\text{F.19e})$$

The main benefit of this formulation compared to (F.7) is that the nonlinear equation (F.19d) is more easily satisfied since the projection in (F.19a) ensures that the initial momentum $\mathbf{p}_{\ell+1/2}$ lies in the cotangent bundle of the manifold, and thus helps ensuring that $\mathbf{q}_{\ell+1}$ stays close to the manifold (we verified this feature numerically). Moreover, as previously mentioned, the component related to the potential $\nabla f(\mathbf{q})$ is integrated exactly in (F.19a) and (F.19e)—recall (F.14) and (F.15). For optimization purposes, we restore the mass $m = h$ —see Eq. (B.2) and Eqs. (3.7)–(3.9)—which only drops the step size in update (F.19c). Note also that here α and β are arbitrary, depending on the dissipation function $\eta(t)$ which is generic—see Eqs. (F.5) and (F.6). Recalling (5.2), we thus have Algorithm 2.

In Algorithm 1 we explicitly set $\eta(t) = \gamma t$, with $\gamma = \text{const.} > 0$, which yields

$$\alpha = e^{-\gamma h/2}, \quad \beta = \cosh(\gamma h/2). \quad (\text{F.20})$$

Instead of tuning γ and h , the method tunes α and h , and then β is fixed as $\beta = \cosh(-\log \alpha)$. Finally, the method (F.19) incorporates equality constraints $\psi_a(\mathbf{q}) = 0$. However, the discussion in Sec. 4 shows that inequality constraints, $\phi_b(\mathbf{q}) \leq 0$, work effectively as equality constraints or do not play a role at all (the associated Lagrange multiplier is set to zero). Accounting for this observation led us to redefine the Jacobian of constraints as in Eq. (5.2), and also the “for” loop between lines 5–11 in Algorithm 2.

F.3 Numerical stability

We provide a linear stability analysis of the integrator (F.19) without constraints for simplicity since the lower bound (3.9) is only known in this setting.⁵ This provides an estimate of the constant C in the step size choice (3.7). Thus, it is sufficient to consider a one-dimensional function $f = \frac{\omega}{2}q^2$. We have

$$p_{\ell+1/2} = \alpha(p_\ell - (h\omega/2)q_\ell), \quad (\text{F.21a})$$

$$q_{\ell+1} = q_\ell + h\beta m^{-1}p_{\ell+1/2}, \quad (\text{F.21b})$$

$$p_{\ell+1} = \alpha p_{\ell+1/2} - (h\omega/2)q_{\ell+1}. \quad (\text{F.21c})$$

Replacing the first update into the subsequent ones we have

$$q_{\ell+1} = (1 - h^2\beta\alpha m^{-1}\omega/2)q_\ell + h\beta\alpha m^{-1}p_\ell, \quad (\text{F.22a})$$

$$p_{\ell+1} = \alpha^2 p_\ell - (h\omega/2)(1 + \alpha^2)q_{\ell+1}. \quad (\text{F.22b})$$

For $\alpha \in (0, 1)$ we have $\alpha\beta < 1$, hence stability requires a bound on the first term in update (F.22a),

$$\left|1 - \frac{h^2 m^{-1} \omega}{2}\right| \leq 1, \quad (\text{F.23})$$

hence

$$\frac{h^2}{m} \leq \frac{4}{\omega}, \quad (\text{F.24})$$

allowing us to choose the step size in (3.7) with a constant $C \leq 2$. We mention that other integrators, e.g., one based on the first order symplectic Euler method would instead give $C \leq \sqrt{2}$. It is interesting that our method, which is based on an integrator of order two and can be traced back to the leapfrog method, yields precisely the maximum step size able to match the lower bound (3.9).

G Optimization over Lie Groups

The reason for transforming the optimization problem (1.1) over the configuration manifold \mathcal{Q} into the constrained optimization problem (1.2) over \mathbb{R}^n is convenience: In general, we want to avoid computing geodesic flows, affine connections, parallel transports, etc., which are numerically prohibitive, specially in higher dimensions. However, there is a particular case of interest where the geodesic flow can be computed efficiently, namely when the configuration manifold is a Lie group, $\mathcal{Q} \equiv \mathcal{G}$.

Many Lie groups have Riemannian metrics that are simple enough to allow tractable computations of parallel transports, while being nontrivial on a global topological level. This is because its tangent space at identity, i.e., its Lie algebra \mathfrak{g} , can be transported around the manifold by the group action, and for Riemannian with sufficiently many symmetries we can find tractable solutions for the geodesic flow on \mathfrak{g} , via the Euler–Arnold equation, and transport the solutions over the manifold.

In this case we can consider an implicit dynamics directly on \mathcal{G} , rather than on some ambient space with constraints. We thus introduce a dissipative flow over a Lie group described by the

⁵The calculation can be done with constraints, but it becomes long and tedious, requiring solving for the Lagrange multipliers.

time-dependent Hamiltonian⁶

$$H = -\frac{1}{4}e^{-\eta(t)} \text{tr}(V^T g^{-1}V) + e^{\eta(t)} f(X) \quad (\text{G.1})$$

with g being a symmetric positive definite constant matrix, $X \in \mathcal{G}$, and $V \in \mathfrak{g}$ plays the role of the velocity/momentum and belongs to the Lie algebra. Note that X and V are (matrix) dynamical variables that evolve in time. The equations of motion over such a matrix Lie group are

$$\dot{X} = e^{-\eta(t)} X g^{-1} V, \quad \dot{V} = -e^{\eta(t)} \text{tr}(\partial_X f(X) X T_a) T_a, \quad (\text{G.2})$$

where $\{T_a\}$ are the generators of the Lie algebra, obeying $[T_a, T_b] = iC_{ab}^c T_c$ and assumed to form an orthogonal basis, $\text{tr}(T_a T_b) \propto \delta_{ab}$. For a practical implementation we actually do not need to use the generators but rather a projection to the Lie algebra,

$$\text{tr}(\partial_X f(X) X T_a) T_a = (\partial_X f(X) X)^T - \partial_X f(X) X. \quad (\text{G.3})$$

Note also that $\partial_X f$ denotes a matrix with entries $(\partial_X f)_{ij} = \partial f / \partial X^{ij}$.

G.1 Dissipative Leapfrog over Lie Groups

Similarly to the derivations in the previous section, we can construct a *presymplectic* integrator for system (G.2) by relying on a symplectic integrator. Consider the dissipative version of RATTLE given by (F.3) but without constraints. In this case the method reduces to the a dissipative version of the leapfrog. We will proceed by analogy to simplify the discussion, although it is not hard to formally justify the following steps. Due to the form of the equations of motion (G.2) let us make the following correspondence:

$$\mathbf{q} \mapsto X, \quad (\text{G.4a})$$

$$\mathbf{p} \mapsto Y, \quad (\text{G.4b})$$

$$\nabla f(\mathbf{q}) \mapsto \text{tr}(\partial_X f(X) X T_a) T_a. \quad (\text{G.4c})$$

The update (F.3c) can be seen as

$$\mathbf{q}(t+h) = \mathbf{q}(t) + (h/2)(e^{-\eta(t)} + e^{-\eta(t+h)})g^{-1}\mathbf{p}(t+h/2) \quad (\text{G.5})$$

and its leading order Lie group analog based on the equations of motion (G.2) reads

$$X(t+h) = X(t) + \frac{h}{2}(e^{-\eta(t)} + e^{-\eta(t+h)})X(t)g^{-1}V(t+h/2) + \dots \quad (\text{G.6})$$

However, this is only the first order expansion of the correct equation obtained by actually exponentiating the Lie algebra,

$$X(t+h) = X(t) \exp \left\{ \frac{h}{2}(e^{-\eta(t)} + e^{-\eta(t+h)})g^{-1}V(t+h/2) \right\}. \quad (\text{G.7})$$

Therefore, with these identifications, we obtain the (unconstrained) Lie group version of the method (F.3) given by

$$V_{\ell+1/2} = V_\ell - (h/2)e^{\eta(t_\ell)} \text{tr}(\partial_X f(X_\ell) X_\ell T_a) T_a, \quad (\text{G.8a})$$

$$t_{\ell+1} = t_\ell + h, \quad (\text{G.8b})$$

$$X_{\ell+1} = X_\ell \exp \left\{ (h/2)(e^{-\eta(t_\ell)} + e^{-\eta(t_{\ell+1})})g^{-1}V_{\ell+1/2} \right\}, \quad (\text{G.8c})$$

$$V_{\ell+1} = V_{\ell+1/2} - (h/2)e^{\eta(t_{\ell+1})} \text{tr}(\partial_X f(X_{\ell+1}) X_{\ell+1} T_a) T_a. \quad (\text{G.8d})$$

⁶The 1/4 factor in the kinetic energy is because we do not require the basis of the Lie algebra to be normalized to have unit norm.

Algorithm 3 DISSLEAPFROGLIE is a presymplectic integrator for solving optimization problems over Lie groups, $\min_{X \in \mathcal{G}} f(X)$. There is a sequence $\{\alpha_\ell\}$, where $\alpha_\ell \in (0, 1)$ (momentum factor), and step size $h > 0$. The parameter β is fixed by Eq. (F.6), and $g \succ 0$ is an arbitrary constant matrix (preconditioner).

```

1: for  $\ell = 0, 1, \dots$  do
2:    $V_{\ell+1/2} \leftarrow \alpha_{\ell+1/2} V_\ell - (h\alpha/2) \operatorname{tr} [\partial_X f(X_\ell) X_\ell T_a] T_a$ 
3:    $X_{\ell+1} \leftarrow X_\ell \exp(\beta_{\ell+1} g^{-1} V_{\ell+1/2})$ 
4:    $V_{\ell+1} \leftarrow \alpha_{\ell+1} V_{\ell+1/2} - (h/2) \operatorname{tr} [\partial_X f(X_{\ell+1}) X_{\ell+1} T_a] T_a$ 
5: end for

```

This is a *dissipative* version of leapfrog for Lie groups. Finally, using the functions introduced in Eqs. (F.5) and (F.6), and further rescaling the velocity/momentum as

$$e^{-\eta(t)} V(t) \rightarrow V(t), \quad (\text{G.9})$$

in analogy with (F.4), we can rewrite the method (G.8) as

$$V_{\ell+1/2} = \alpha_{\ell+1/2} V_\ell - (h\alpha_{\ell+1/2}/2) \operatorname{tr} (\partial_X f(X_\ell) X_\ell T_a) T_a, \quad (\text{G.10a})$$

$$X_{\ell+1} = X_\ell \exp(h\beta_{\ell+1} g^{-1} V_{\ell+1/2}), \quad (\text{G.10b})$$

$$V_{\ell+1} = \alpha_{\ell+1} V_{\ell+1/2} - (h/2) \operatorname{tr} (\partial_X f(X_{\ell+1}) X_{\ell+1} T_a) T_a. \quad (\text{G.10c})$$

The same previous comment regarding the mass $m = h$ applies for solving optimization problems. Note also that we use formula (G.3) in place of the trace, so computations can be done in global coordinates, i.e., we do not need to parametrize the group in terms of the generators, which is quite convenient in practice. We thus state Algorithm 3.

Although α and β are associated to a generic damping function $\eta(t)$, one can use the constant case $\eta(t) = \gamma t$ as in Eq. (F.20). Recall also that we can use formula (G.3) to compute the trace, without generators. Moreover, “exp” refers to the matrix exponential, which defines a map from the Lie algebra to the Lie group. This exponential can be replaced by any structure-preserving (symplectic) approximation such as a Cayley transform,

$$\exp(hY) = \left(I - \frac{h}{2}Y\right)^{-1} \left(I + \frac{h}{2}Y\right) + \mathcal{O}(h^3). \quad (\text{G.11})$$

Importantly, Algorithm 3 can also be applied to naturally reductive *homogeneous spaces*, which include:

- Stiefel manifolds.
- Grassmannian manifolds.
- The space of positive definite matrices (and their complex analogues).
- Projective spaces.
- Affine spaces.

This is because we can view Hamiltonian systems on homogeneous spaces as reduced mechanics obtained by Hamiltonian systems with symmetries on associated Lie groups. Concretely, we simply need to restrict the momentum to a vector space complementary to the Lie algebra of the isotropy group, as discussed in the context of sampling [42].

H Numerical Details for SSK

The problem (6.2) is over a hypersphere, with the constraint in the form

$$\psi(\boldsymbol{\sigma}) = \|\boldsymbol{\sigma}\|^2 - n = 0. \quad (\text{H.1})$$

Note that $\mathbf{q} \equiv \boldsymbol{\sigma}$ in our notation. Thus, the Jacobian matrix of constraints is simply $\mathcal{J}(\boldsymbol{\sigma})^T = 2\boldsymbol{\sigma}$, and the gradient of the objective function is $\nabla\mathcal{H}(\boldsymbol{\sigma}) = -M\boldsymbol{\sigma} - \rho\mathbf{g}$. In fact, the constraint (H.1) can be solved in closed form. Consider Algorithm 1 and denote

$$\mathbf{q}_{\ell+1} = \mathbf{a} + \lambda\mathbf{b}, \quad (\text{H.2})$$

where $\mathbf{a} \equiv \mathbf{q}_\ell + \beta g^{-1}\mathbf{p}_\ell$, $\mathbf{b} \equiv (\beta h\alpha/2)g^{-1}\mathcal{J}(\mathbf{q}_\ell)$, and $\lambda \equiv \lambda_\ell$. Note that in this case the Lagrange multiplier is a scalar. Solving (H.1) for λ , i.e., computing line 7 in Algorithm 1, requires solving

$$\|\mathbf{a} - \lambda\mathbf{b}\|^2 - n = \|\mathbf{b}\|^2\lambda^2 - 2\mathbf{a} \cdot \mathbf{b}\lambda + (\|\mathbf{a}\|^2 - n) = 0, \quad (\text{H.3})$$

whose exact solution is (we should take the smallest root)

$$\lambda_\ell = \frac{\mathbf{a} \cdot \mathbf{b} - \sqrt{\Delta}}{\|\mathbf{b}\|^2}, \quad \Delta \equiv (\mathbf{a} \cdot \mathbf{b})^2 - \|\mathbf{b}\|^2(\|\mathbf{a}\|^2 - n). \quad (\text{H.4})$$

We use this exact formula when solving problem (6.2) with Algorithm 1.⁷

In the examples of Fig. 2 (Sec. 6) we initialize at $\mathbf{q}_0 = \boldsymbol{\sigma}_0 = \mathbf{1}$, which is on the n -sphere. The momentum is always initialized at $\mathbf{p}_0 = \mathbf{0}$. Those examples show a single run of Algorithm 1 in comparison with gradient flow [7] (Riemannian gradient descent). However, we verified similar results for several instances of the problem as well. Note that the problem is of dimension $n = 1000$, which is significantly high dimensional and this example provides a real benchmark.

To provide error quantification of our method, we consider 100 Monte Carlo runs of Algorithm 1 and gradient flow, both with step size $h = 0.5/\lambda_{\max}(M)$. We fix the momentum factor as $\alpha = 0.9$. We consider random initializations, where we choose one component of $\boldsymbol{\sigma}_0$ at random, say the i th component, and set it to $\sigma_0^i = \sqrt{n}$, while the remaining components are $\sigma_0^j = 0$ for $j \neq i$. We run both methods up to a tolerance error of 10^{-10} (which provides a relative error with respect to the minimum of the objective function of $\sim 10^{-14}$). We consider problem (6.1) with $\rho = 0$ (no external field) in $n = 500$ dimensions, which is large. We show in Fig. 3 (left) a histogram of the number of iterations. All methods, and in all instances of the problem, converged successfully to the required accuracy. Note, however, that Algorithm 1 is consistently faster than gradient flow by orders of magnitude.

Next, for a fixed instance of the problem in $n = 200$ dimensions, as described in the previous paragraph, we fix $\alpha = 0.9$ and consider a step size $h = C/\lambda_{\max}(M)$, where we vary $C \in [0.1, 2]$. We require all algorithms to achieve a tolerance error $\sim 10^{-7}$ in the relative error of the objective function value with respect to the optimum. We show in Fig. 3 (right) a plot of this relative error against C . Note how Algorithm 1 is considerable more stable than gradient flow (Riemannian gradient descent). We repeated this experiment for several instances of the problem, obtaining identical results as the one displayed.

Finally, we now vary both parameters α and the step size h into Algorithm 1 for an instance of problem (6.2) (with $\rho = 0$, no external field) in $n = 100$ dimensions. This allows us to find

⁷As a sanity check, we compared this exact procedure with a numerical solution of the constraint (H.1) via Newton-Raphson method. The results were in complete agreement.

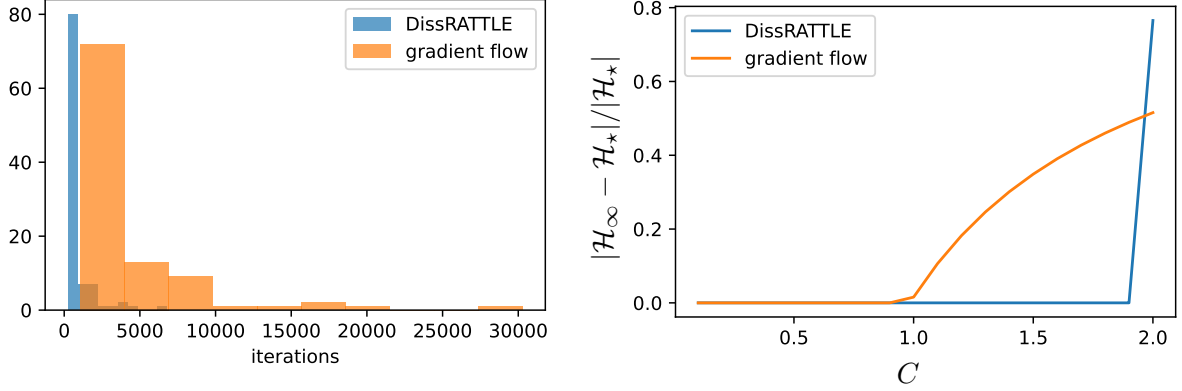


Figure 3: *Left:* 100 Monte Carlo runs with random initializations on a problem of dimension $n = 500$. We report histograms of the number of iterations such that both algorithms achieved a relative error $\sim 10^{-14}$ in the objective function value. Algorithm 1 is much faster than gradient flow (Riemannian gradient descent [7]). Both methods used the same step size, favoring gradient flow. *Right:* Plot of the relative error against C , where $h = C/\lambda_{\max}(M)$. Note that Algorithm 1 is almost twice times more stable than gradient flow, even though it is “accelerated.”

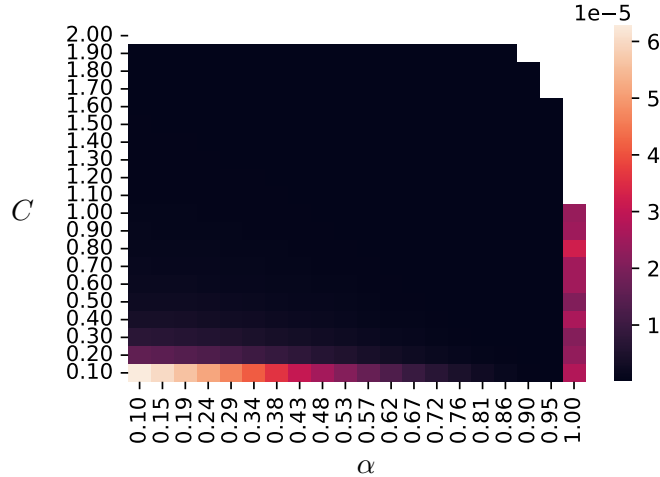


Figure 4: We vary the parameter $\alpha \in (0,1)$ and the step size $h = C/\lambda_{\max}(M)$, with $C \in (0,2)$, into Algorithm 1 for an instance of problem (6.2). The heatmap is the value of the relative error $|\mathcal{H}_\infty - \mathcal{H}_*|/|\mathcal{H}_*|$. The white area corresponds to cases where the algorithm did not converge.

the stability region of the method in the parameter space. The results are shown in the heatmap of Fig. 4. For the majority of parameter choices the algorithm converged successfully. Only for very large values of $C \simeq 2$ the method diverged (white area), or when the method was very weakly damped, $\alpha \simeq 1$. Interestingly, the method converged even for large values of α . The entire dark region corresponds to values of the relative error of $\sim 10^{-6}$, according to our chosen tolerance error. We repeated this experiment for few other instances of the problem, with no noticeable change in the results. Therefore, Algorithm 1 proved to be quite stable.

H.1 SSK over $SO(n)$

It is possible to redefine problem (6.1)/(6.2) over a homogenous space. This is done as

$$\mathcal{H}(X) = -\frac{1}{2} \sum_{i,j=1}^n X_{i1} M^{ij} X_{j1} - \rho \sum_{i=1}^n g^i X_{i1} \quad (\text{H.5})$$

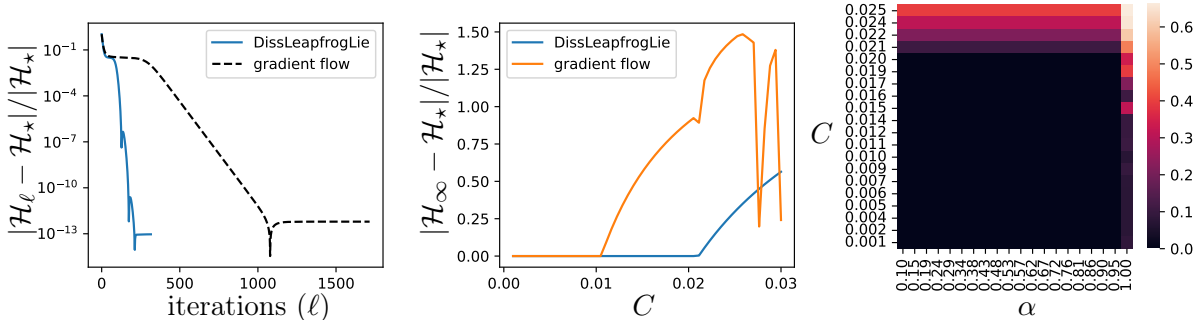


Figure 5: Solving problem (H.6) with Algorithm 3 and Riemannian gradient descent (gradient flow) [7]. *Left:* We choose $n = 500$, $\alpha = 0.9$, and step size $h = 0.001/\lambda_{\max}(M)$ so gradient flow could converge. *Middle:* We vary the step size $h = C/\lambda_{\max}(M)$. Note how Algorithm 3 is twice more stable. *Right:* Heat map of the relative error in the objective function by varying α and C for Algorithm 3. The method was able to converge for a large range of values in the parameter space.

where $X \in SO(n)$, the special orthogonal group. This is because the oriented sphere can be written as $\mathcal{S}_{n-1} \equiv SO(n)/SO(n-1)$. We can thus find the ground state of an SSK model by an optimization problem over the $SO(n)$ group,

$$\min_{X \in SO(n)} \mathcal{H}(X). \quad (\text{H.6})$$

We apply Algorithm 3 to this problem, with $\rho = 0$ (no external field) and damping $\eta(t) = \gamma t$; see Eq. (F.20). Similar results are obtained for an external field, $\rho \neq 0$. We compare this method with Riemannian gradient descent [7] (“gradient flow”), when the geodesic flow is computed over the Lie group. In Fig. 5 (left) we show an instance of this problem. We can see that Algorithm 3 is significantly faster, besides being more stable (middle plot). We show the stability of the method on parameter space (right plot); the heatmap has values $|\mathcal{H}_\infty - \mathcal{H}_\star|/|\mathcal{H}_\star|$.

In high dimensions, applying the constrained method in Algorithm 1 is more efficient than the matrix approach of Algorithm 3. To illustrate this, in Fig. 6 we compare both methods when applied to the same SSK problem and with the same initial condition. We vary the size n of the problem. For both methods we set $\alpha = 0.9$. The step sizes were chosen so that both methods achieved approximately the same tolerance error during the same number of iterations. For Algorithm 1 we set $h = 1/\lambda_{\max}(M)$ and for Algorithm 3 we set $h = 0.005/\lambda_{\max}(M)$. However, Algorithm 3 became unstable for larger problem sizes (with this step size choice), while Algorithm 1 did not and in fact could operate with even larger step sizes. Overall, we believe the approach through constrained optimization is superior and more scalable whenever the problem can be vectorized efficiently.

I Orthogonal Procrustes Problem

We consider the problem

$$\min_{X \in SO(n)} \|M - X\|_F^2, \quad (\text{I.1})$$

where M is a given matrix. Note that the constraints are $X^T X = X X^T = I$ and $\det X = +1$, so this is a *nonconvex* problem. This is a generalization of the famous orthogonal Procrustes problem, which relaxes the condition $\det X = +1$; it has several applications in statistics, multidimensional scaling, and natural language processing [43]. Problem (I.1) is also known as

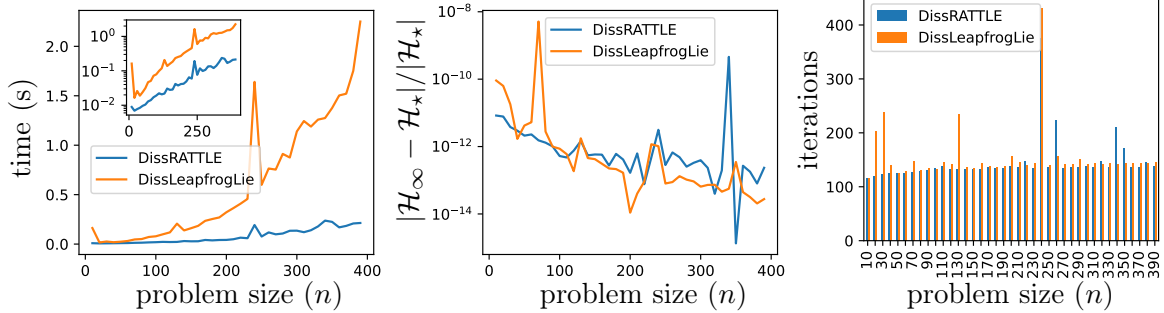


Figure 6: Comparing Algorithms 1 and 3 when solving the SSK problem. *Left:* Wall-clock time vs. n . The inset shows the y -axis in log scale. Note how Algorithm 1 is more scalable and also stable. Algorithm 3 diverged for higher n (with this choice of step size), contrary to Algorithm 1 which could operate with even larger step sizes. *Middle:* We show the relative error of the objective function to confirm that both methods achieved the same accuracy in the solution. *Right:* We also show the number of iterations, which is also similar for both methods with this choice of parameters.

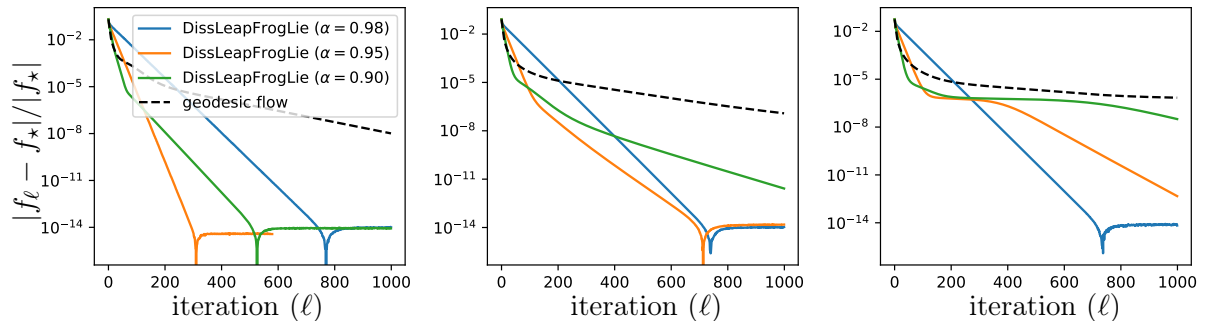


Figure 7: Solving problem (I.1) with Algorithm 3 and Riemannian gradient descent (gradient flow). In all cases we sample $M_{ij} \sim \mathcal{N}(0, 1)$. *Left:* Problem with dimension $n = 100$. *Middle:* $n = 500$. *Right:* $n = 1000$. If we carefully tune α and h in Algorithm 3 the convergence is even faster than shown in these plots. Note how the convergence of gradient flow is quite slow, specially for large n .

Wahba’s problem [44]. There is a closed form solution to this problem, which however involves computing an SVD: $X_* = UDV^T$, where $M = U\Sigma V^T$, and $D_{ij} = 0$ for $i \neq j$, $D_{ii} = 1$ for $i = 1, \dots, n - 1$, and $D_{nn} = \det(UV^T)$.

Problem (I.1) is well-suited to Algorithm 3, whose implementation becomes extremely simple. We thus compare this method with Riemannian gradient descent (gradient flow), for a few values of n . We choose three different values of α to illustrate the role of the momentum factor. The results are shown in Fig. 7 for a single run of these algorithms, with initialization $X_0 = I$. The step size of all methods is chosen as $h = \frac{1}{2}\lambda_{\max}(M)$, which allowed gradient flow to converge; Algorithm 3 allows much larger step sizes however, which makes its convergence faster than shown in these plots. Note how gradient flow gets stalled, specially with increasing dimensionality. Next, In Fig. 8, we consider 100 Monte Carlo runs for $n = 100$ and show histograms of the number of iterations and the relative error in the objective function, running both methods until achieving a tolerance error $\approx 10^{-8}$ in the solution. In Fig. 9 we illustrate the improved stability of Algorithm 3 compared to Riemannian gradient descent.

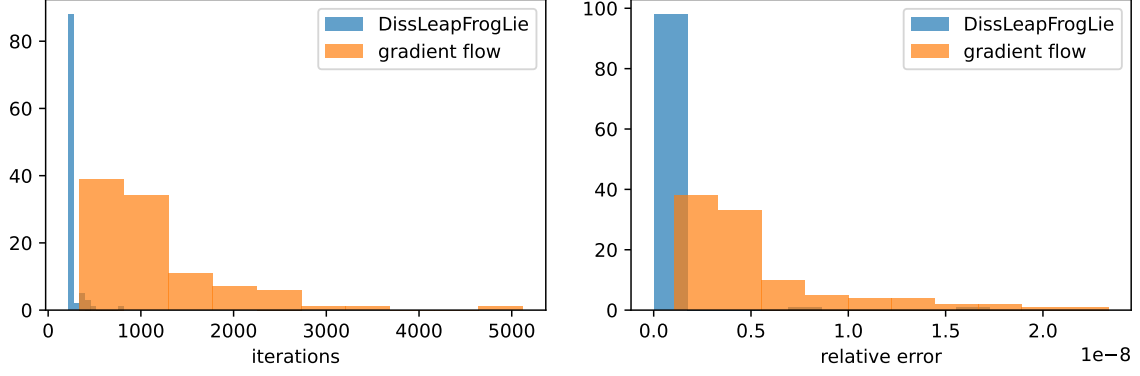


Figure 8: We consider 100 Monte Carlo runs on problem (I.1) in $n = 100$ dimensions, with Algorithm 3 ($\alpha = 0.95$) and Riemannian gradient descent; both with step size $h = \frac{1}{2}\lambda_{\max}(M)$. *Left:* Histogram of the number of iterations for convergence up to a tolerance error $\approx 10^{-8}$. *Right:* Histogram of the relative error of the final iteration. Note how Algorithm 3 converges in a much smaller number of iteration, and to a more accurate solution.

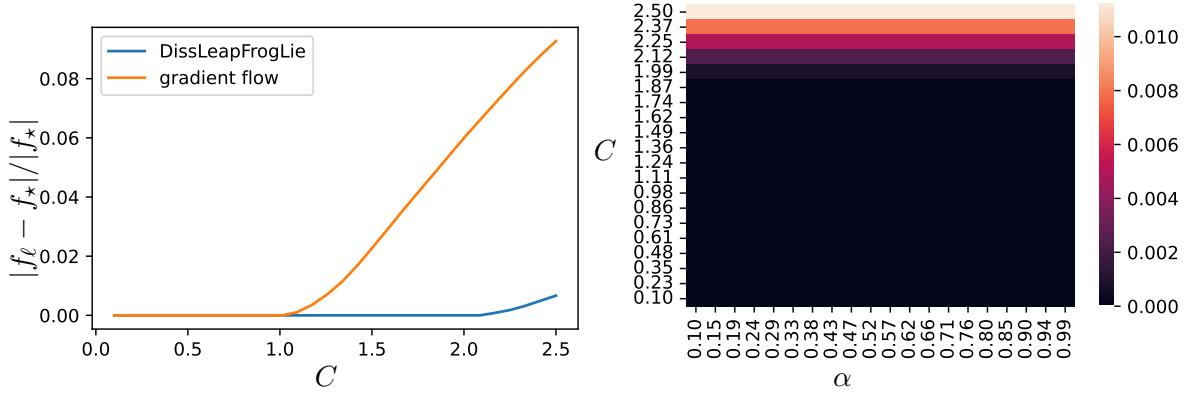


Figure 9: Problem (I.1) in $n = 50$ dimensions. *Left:* We set $\alpha = 0.95$ into Algorithm 3 and vary $C \in (0, 2.5)$ for step size $h = C\lambda_{\max}(M)$. Note how Algorithm 3 is much more stable than gradient flow. *Right:* For another instance of the problem, we check the stability of Algorithm 3 by varying C and α ; the heatmap shows values of the achieved relative error of the objective function after convergence up to tolerance 10^{-8} (in the state variable) or 2000 iterations.

References

- [1] P. A. M. Dirac, “Generalized Hamiltonian dynamics,” *Canadian J. of Math.* **2** (1950) 129–148.
- [2] P. A. M. Dirac, *Lectures on Quantum Mechanics*. Dover Publications, 2001.
- [3] M. Henneaux and C. Teitelboim, *Quantization of Gauge Systems*. Princeton University Press, 1994.
- [4] P. A. Absil, R. Mahony, and R. Sepulchre, *Optimization Algorithms on Matrix Manifolds*. Princeton University Press, 2008.
- [5] N. Boumal, *An Introduction to Optimization on Smooth Manifolds*. Cambridge University Press, 2023.
- [6] C. Criscitiello and N. Boumal, “An accelerated first-order method for non-convex optimization on manifolds,” *Found. Comput. Math.* (2022) .

- [7] H. Zhang and S. Sra, “First-order methods for geodesically convex optimization,” *Conf. Learning Theory* (2016) 1617–1638.
- [8] J. Townsend, N. Koep, and S. Weichwald, “Pymanopt: A Python toolbox for optimization on manifolds using automatic differentiation,” *J. Mach. Learn. Res.* **17** (2016) 1–5.
- [9] K. Ahn and S. Sra, “From Nesterov’s estimate sequence to Riemannian acceleration,” *Conf. Learning Theory* (2020) 84–118.
- [10] F. Alimisis, A. Orvieto, G. Becigneul, and A. Lucchi, “Momentum improves optimization on Riemannian manifolds,” *AISTATS* **130** (2021) 1351–1359.
- [11] R. Berndt, *An Introduction to Symplectic Geometry*. American Mathematical Society, 2000.
- [12] A. Wibisono, A. C. Wilson, and M. I. Jordan, “A variational perspective on accelerated methods in optimization,” *Proc. Nat. Acad. Sci.* **113** no. 47, (2016) E7351–E7358.
- [13] G. França, J. Sulam, D. P. Robinson, and R. Vidal, “Conformal symplectic and relativistic optimization,” *J. Stat. Mech.* **2020** no. 12, (2020) 124008.
- [14] M. Betancourt, M. I. Jordan, and A. Wilson, “On symplectic optimization,” [arXiv:1802.03653](https://arxiv.org/abs/1802.03653) [stat.CO].
- [15] M. Muehlebach and M. I. Jordan, “Optimization with momentum: dynamical, control-theoretic, and symplectic perspectives,” *J. Mach. Learn. Res.* **22** no. 73, (2021) 1–50.
- [16] A. Bravetti, M. L. Daza-Torres, H. Flores-Arguedas, and M. Betancourt, “Optimization algorithms inspired by the geometry of dissipative systems,” [arXiv:1912.02928](https://arxiv.org/abs/1912.02928) [math.OC].
- [17] G. França, D. P. Robinson, and R. Vidal, “Gradient flows and proximal splitting methods: A unified view on accelerated and stochastic optimization,” *Phys. Rev. E* **103** (2021) 053304.
- [18] G. França, D. P. Robinson, and R. Vidal, “A nonsmooth dynamical systems perspective on accelerated extensions of ADMM,” *IEEE Trans. Automatic Control* **68** no. 5, (2023) 2966–2978.
- [19] G. Benettin and A. Giorgilli, “On the Hamiltonian interpolation of near-to-the-identity symplectic mappings with application to symplectic integration algorithms,” *J. Stat. Phys.* **74** (1994) 1117–1143.
- [20] R. I. McLachlan and G. R. W. Quispel, “Splitting methods,” *Acta Numer.* **11** (2002) 341.
- [21] B. Leimkuhler and S. Reich, *Simulating Hamiltonian Dynamics*. Cambridge University Press, 2004.
- [22] R. I. McLachlan, G. Quispel, and W. Reinout, “Geometric integrators for ODEs,” *J. Phys. A: Math. and Gen.* **39** no. 19, (2006) 5251.
- [23] E. Hairer, C. Lubich, and G. Wanner, *Geometric Numerical Integration: Structure-Preserving Algorithms for Ordinary Differential Equations*. Springer, 2010.

- [24] G. França, M. I. Jordan, and R. Vidal, “On dissipative symplectic integration with applications to gradient-based optimization,” *J. Stat. Mech.* **2021** no. 4, (2021) 043402.
- [25] M. J. Gotay, J. M. Nester, and G. Hinds, “Presymplectic manifolds and the Dirac–Bergmann theory of constraints,” *J. Math. Phys.* no. 19, (1978) 2388.
- [26] J. E. Marsden and M. West, “Discrete mechanics and variational integrators,” *Acta Numer.* **10** (2001) 357–514.
- [27] Y. Nesterov, *Lectures on convex optimization*. Springer, 2018.
- [28] H. C. Andersen, “Rattle: A “velocity” version of the SHAKE algorithm for molecular dynamics calculations,” *J. Comput. Phys.* **52** no. 1, (1983) 24–34.
- [29] B. J. Leimkuhler and R. D. Skeel, “Symplectic numerical integrators in constrained Hamiltonian systems,” *J. Comput. Phys.* **112** (1994) 117–125.
- [30] S. Reich, “Symplectic integration of constrained Hamiltonian systems by composition methods,” *SIAM J. Numer. Anal.* **32** no. 3, (1996) 475–491.
- [31] B. Leimkuhler and C. Matthews, “Efficient molecular dynamics using geodesic integration and solvent–solute splitting,” *Proc. Royal Soc. A: Math., Phys. and Eng. Sci.* **472** no. 2189, (2016) 20160138.
- [32] J. Baik, E. Collins-Woodfin, P. L. Doussal, and H. Wu, “Spherical spin glass model with external field,” *J. Stat. Phys.* **183** no. 31, (2021) .
- [33] V. I. Arnold, A. Weinstein, and K. Vogtmann, *Mathematical Methods of Classical Mechanics*. Springer, 1989.
- [34] J. E. Marsden and T. S. Ratiu, *Introduction to Mechanics and Symmetry: A Basic Exposition of Classical Mechanical Systems*. Springer, 2010.
- [35] S. M. Carroll, *Spacetime and Geometry: An Introduction to General Relativity*. Cambridge University Press, 2019.
- [36] M. Nakahara, *Geometry, Topology, and Physics*. IOP Publishing, 2003.
- [37] H. Marthinsen and B. Owren, “Geometric integration of non-autonomous Hamiltonian problems,” *Adv. Comput. Math.* **42** (2016) 313–332.
- [38] M. Asorey, J. F. Cariñena, and L. A. Ibort, “Generalized canonical transformations for time-dependent systems,” *J. Math. Phys.* **24** no. 12, (1983) 2745–2750.
- [39] A. C. Hansen, “A theoretical framework for backward error analysis on manifolds,” *J. Geom. Mech.* **3** no. 1, (2011) 81–111.
- [40] S. Wiggins, *Introduction to Applied Nonlinear Dynamical Systems and Chaos*. Springer, 2000.
- [41] P. Hartman, “A lemma in the theory of structural stability of differential equations,” *Proc. Amer. Math. Soc.* **11** (1960) 610–620.
- [42] A. Barp, A. Kennedy, and M. Girolami, “Hamiltonian Monte Carlo on symmetric and homogeneous spaces via symplectic reduction,” [arXiv:1903.02699](https://arxiv.org/abs/1903.02699) [stat.CO].
[arXiv:1903.02699v2](https://arxiv.org/abs/1903.02699v2) [stat.CO].

- [43] J. C. Gower and G. B. Dijksterhuis, *Procrustes Problems*. Oxford University Press, 2004.
- [44] G. Wahba, "A least squares estimate of satellite attitude," *SIAM Review* **7** no. 3, (1965) 409–409.